Microbiological Research 294 (2025) 128097

Contents lists available at ScienceDirect

Microbiological Research

journal homepage: www.elsevier.com/locate/micres

Identification of a novel forkhead transcription factor MtFKH1 for cellulase and xylanase gene expression in *Myceliophthora thermophila* (ATCC 42464)

Yapeng Lai [a,b], Juan Wang [a], Ning Xie [a], Gang Liu [a,*], Donnabella Castillo Lacap-Bugler [b,*]

[a] Shenzhen Key Laboratory of Microbial Genetic Engineering, College of Life Sciences and Oceanography, Shenzhen University, Shenzhen 518055, China
[b] School of Science, Faculty of Health and Environmental Science, Auckland University of Technology, Auckland 1010, New Zealand

ARTICLE INFO

Keywords:
Myceliophthora thermophila
Cellulase
Xylanase
Forkhead transcription factor
CRISPR/Cas9
Comparative transcriptome

ABSTRACT

Myceliophthora thermophila is a thermophilic fungus, known to produce industrially important enzymes in biorefineries. The mechanism underlying cellulase and xylanase expression in filamentous fungi is a complex regulatory network controlled by numerous transcription factors (TFs). These TFs in *M. thermophila* remain unclear. Here, we identified and characterised a novel cellulase and xylanase regulator MtFKH1 in *M. thermophila* through comparative transcriptomic and genetic analyses. Five of the eight potential TFs, which showed differential expression levels when grown on Avicel and glucose, were successfully deleted using the newly designed CRISPR/Cas9 system. This system identified the forkhead TF MtFKH1. The disruption of *Mtfkh1* elevated the cellulolytic and xylanolytic enzyme activities, whereas the overexpression of *Mtfkh1* led to considerable decrease in cellulase and xylanase production in *M. thermophila* cultivated on Avicel. The loss of *Mtfkh1* also exhibited an impairment in sporulation in *M. thermophila*. Real-time quantitative reverse transcription PCR (RT-qPCR) and the electrophoretic mobility shift assays (EMSAs) demonstrated that MtFKH1 regulates the gene expression and specifically bind to the promoter regions of genes encoding β-glucosidase (*bgl1/MYCTH_66804*), cellobiohydrolase (*cbh1/MYCTH_109566*), and xylanase (*xyn1/MYCTH_112050*), respectively. Furthermore, DNase I footprinting analysis identified binding motif of MtFKH1 in the upstream region of *Mtbgl1*, with strongest binding affinity. Finally, transcriptomic profiling and Gene Ontology (GO) enrichment analyses of *Mtfkh1* deletion mutant revealed that the regulon of MtFKH1 were significantly prevalent in hydrolase activity (acting on glycosyl bonds), polysaccharide binding, and carbohydrate metabolic process functional categories. These findings expand our knowledge on how forkhead transcription factor regulates lignocellulose degradation and provide a novel target for engineering of fungal cell factories with the hyperproduction of cellulase and xylanase.

1. Introduction

Lignocellulosic biomass has been regarded as a promising alternative raw material for biofuels and value-add biochemicals production (Rubin, 2008; Agrawal et al., 2021). The biological depolymerisation of lignocellulose requires at least two main enzymes: cellulase and hemicellulase (Sanchez, 2009). Cellulase includes endo-β-1,4-glucanase (EGs; EC 3.2.1.4), cellobiohydrolase (CBHs; EC 3.2.1.91), and β-glucosidase (BGLs; EC 3.2.1.21). Hemicellulase mainly consists of endo-1, 4-β-xylanase (EC 3.2.1.8), β-xylosidase (EC 3.2.1.37), along with other hydrolases and esterases (Gupta et al., 2016). The cellulase and xylanase act synergistically to hydrolyze lignocellulose into glucose and xylose, which are utilized to generate bioethanol and biochemicals by microbial fermentation (Gupta et al., 2016; Taha et al., 2016). These important enzymes have been applied in a variety of manufacturing processes in different industries including textile and detergent, paper pulp bleaching, food and feed, and pharmaceutical and nutraceutical industry (Juturu and Wu, 2014; Mendonca et al., 2023).The increased demand in the production of bioethanol and biochemicals from lignocellulosic biomass has placed cellulase and xylanase at the forefront of biorefinery processes, which necessitates exploring cost-efficiency in converting lignocellulosic biomass into fermentable sugars via enzymatic hydrolysis (Singhania et al., 2010; Bajaj and Mahajan, 2019; Liu et al., 2020). Nevertheless, the high cost of lignocellulose degrading enzymes is still a bottleneck for the commercial production of lignocellulosic biofuels to date (Liu et al., 2019a, 2019b; Sperandio and Filho, 2021).

Filamentous fungi are potent lignocellulolytic enzymes producers and have been utilized to produce a broad spectrum of enzymes mixes

* Corresponding authors.
E-mail addresses: zjuliug@szu.edu.cn (G. Liu), dlacapbu@aut.ac.nz (D.C. Lacap-Bugler).

https://doi.org/10.1016/j.micres.2025.128097
Received 5 December 2024; Received in revised form 7 February 2025; Accepted 10 February 2025
Available online 14 February 2025

employed in diverse biotechnological applications (Berlin, 2013; Makela et al., 2014). Thermophilic fungi have been receiving considerable interest for the bioconversion of lignocellulosic biomass into cellulosic ethanol since they are a significant source of industrially thermostable enzymes (Morgenstern et al., 2012; Basotra et al., 2016). The advantages of using thermostable cellulases at elevated temperatures include higher hydrolysis rates, better substrate solubility and lower viscosity, and decreased risk of microbial contamination when compared with enzymes from mesophilic species (Yeoman et al., 2010; Blumer-Schuette et al., 2014; Ajeje et al., 2021). *Myceliophthora thermophila* is a thermophilic filamentous fungus that grows optimally at temperatures between 45°C and 50°C and offers a complete array of carbohydrate-active enzymes (CAZymes) necessary for the decomposition of plant cell wall polysaccharides (Karnaouri et al., 2014). Currently, *M. thermophila* is attracting particular attention for its potential as an industrial factory for chemicals and biofuels production, since its genome, transcriptome and secretome are well annotated and accessible (Berka et al., 2011; Kolbusz et al., 2014). However, the production levels of biomass degrading enzymes from this fungal species are typically low compared with those regularly used mesophilic counterparts such as *Trichoderma* spp. and *Aspergillus* spp. (Berka et al., 2011; Singh, 2016). Therefore, extensive research has focused on improving the lignocellulolytic enzymes production in *M. thermophila* (Dos Santos Gomes et al., 2019; Li et al., 2020a, 2020b).

In filamentous fungi, the expression of lignocellulolytic enzyme encoding genes is strictly regulated by a battery of transcriptional activators and repressors, and efficient manipulation of these key regulators will improve the production of the extracellular enzymes (Benocci et al., 2017; Adnan et al., 2022). XlnR is the first identified transcription factor involved in regulating the expression of xylanolytic and cellulolytic enzyme genes induced by xylose or xylan in *Aspergillus niger* (van Peij et al., 1998). Since then, several transcription regulators involved in lignocellulose degradation have been characterized, including the transcriptional activators CLR-1, CLR-2, CLR-4, Ace2, Ace3, Ace4, and Vib-1, and the transcriptional repressors Cre1, Ace1 (Alazi and Ram, 2018; Zhao et al., 2023). All of which are engaged in the regulation of cellulolytic and/or hemicellulolytic enzyme production. The XlnR orthologs in *Trichoderma reesei* (Xyr1) and *Aspergillus oryzae* (XlnR) are essential for the synthesis of both cellulase and hemicellulase, while XLR-1 in *Neurospora crassa* and XlnR in *Aspergillus nidulans* are required only for hemicellulase gene expression (Marui et al., 2002; Stricker et al., 2006; Sun et al., 2012; Klaubauf et al., 2014). In *N. crassa*, CLR-1, CLR-2 are indispensable regulators of cellulase expression, as CLR-2 homologs in *A. nidulans* (ClrB), and *Penicillium oxalicum* (ClrB) but not in *T. reesei* (Coradetti et al., 2012; Hakkinen et al., 2014; Craig et al., 2015; Li et al., 2015). In *T. reesei*, Ace1 acts as a repressor of both cellulase and xylanase production, as the deletion of which led to an enhancement in the expression of all the major cellulase and two hemicellulase genes (Saloheimo et al., 2000; Aro et al., 2003). In contrast, the lack of Ace2 in *T. reesei* resulted in reduced expression of genes encoding for cellulases and xylanase when grown in cellulose media (Aro et al., 2001). Whilst Ace3 acts as positive regulator of cellulase and xylanase, which regulates the target genes directly and indirectly via modulating *xyr1* transcription in *T. reesei* (Hakkinen et al., 2014). The Zn(II)$_2$Cys$_6$ transcription factor CLR-4 plays a pivotal role in the regulation of cellulolytic gene expression and directly regulates the expression of CLR-1 by binding to the promoter regions of *clr-1* gene in *N. crassa* (Liu et al., 2019d). Furthermore, the newly reported Ace4 is identified as an activator involved in the regulation of genes responsible for encoding cellulase, and overexpression of *ace4* elevated cellulase production by 22 % under cellulose-induced cultivation of *T. reesei* (Chen et al., 2021). The deletion of Cre1(encodes carbon catabolite repressor protein), which is a homolog of Mig1 in *Saccharomyces cerevisiae*, increased cellulolytic activity and upregulated the transcription of cellulolytic genes in the presence of cellulose in *N. crassa* (Sun and Glass, 2011). Moreover, overexpression of regulatory gene *vib-1* considerably improved cellulase production and protein secretion in *T. reesei* (Zhang et al., 2018).

In *M. thermophila*, a few transcription factors associated with lignocellulosic biomass degradation have also been identified. One transcriptional activator MtXyr1 and another transcriptional repressor MtCre1, which are involved in regulation of the expression of hemicellulolytic, or cellulolytic genes have been characterized in *M. thermophila* (Wang et al., 2015; Yang et al., 2015). Overexpression of MtXyr1 under the control of the strong constitutive *pdc* (pyruvate decarboxylase) promoter resulted in 9-fold higher xylanase activity in corncob-containing medium and exhibited less effects on the cellulase activities while RNA interference of MtCre1 caused increased cellulolytic activity and expression level of cellulolytic genes under inducing conditions. In addition, MtXyr1 also controls the expression of genes engaged in pentose transport and catabolism (Dos Santos Gomes et al., 2019). Similar to its homolog CLR-4 in *N. crassa*, MtCLR-4 plays key role in the regulation of genes encoding (hemi-)cellulases through directly regulating the expression of the crucial transcription activators MtCLR-2 and MtXyr1, and *Mtcr-1* encoding adenylyl cyclase in the cAMP signaling pathway (Liu et al., 2019d). Recently, a novel transcriptional factor MtCLR-5 was found to be critical for cellulose depolymerization in *M. thermophila*, the deletion of this TF encoding gene decreased the endoglucanase activity and protein secretion when cultivated in cellulose media (Xue et al., 2023). However, to-date the gene expression system of lignocellulolytic enzymes is limited in *M. thermophila*, and more transcription factors involved in the regulatory network controlling plant biomass degradation remains to be elucidated.

The forkhead transcription factors, which contain the typical forkhead box (Fox) or winged helix DNA-binding domain (Korver et al., 1997), are crucial regulators that control development, cell cycle, signal transduction, morphogenesis, and metabolism regulation (Carlsson and Mahlapuu, 2002). Forkhead proteins are conserved in yeast, filamentous fungi as well as in mammals. Some members from this protein family have been characterized, including ScFKH1 and ScFKH2 in *S. cerevisiae* (Hollenhorst et al., 2000; Zhu et al., 2000), HcFKH1 in *Hapsidospora chrysogena* (formerly *Acremonium chrysogenum*) (Schmitt et al., 2004), PrFKH1 in *Penicillium rubens* (formerly *Penicillium chrysogenum*) (Dominguez-Santos et al., 2015), PoX08522 in *Penicillium oxalicum* (Zhao et al., 2016), AnFKHB in *Aspergillus nidulans* (Jang et al., 2023), and FOXOs in humans (Bach et al., 2018; Laissue, 2019). However, the regulatory role of forkhead proteins in lignocellulose degrading enzymes production in *M. thermophila* remains largely unknown.

In the current study, a novel transcriptional factor in *M. thermophila* was identified through comparative transcriptomic and molecular genetics analyses. Here, the key regulator gene, *Mtfkh1* in *M. thermophila* ATCC 42464, encoding a forkhead protein that negatively regulates the expression of major cellulase and xylanase genes by directly binding to their promoter regions was described. To the best of our knowledge, MtFKH1 is the first characterized member of the forkhead protein family in *M. thermophila*, which enriches our understanding of the regulation of lignocellulose degradation in filamentous fungi.

2. Materials and methods

2.1. Strains and culture conditions

Myceliophthora thermophila (ATCC 42464) was used as the parental strain throughout this study. The *M. thermophila* strains were cultured on potato dextrose agar (PDA) plates at 45℃ for 7 days to obtain asexual spores (conidia), which were suspended with 0.2 % (v/v) Tween-80 solution to prepare spore suspensions. For mycelial growth (for DNA extraction), the fungi were cultured in Mandels medium (Wang et al., 2015) [(g/L) $(NH_4)_2SO_4$, 1.4; Urea, 0.3; KH_2PO_4, 2.0; $MgSO_4{\cdot}7\,H_2O$, 0.3; $CaCl_2{\cdot}2\,H_2O$, 0.4; $FeSO_4{\cdot}7\,H_2O$, 0.005; $ZnSO_4{\cdot}7\,H_2O$, 0.0017; $CoCl_2{\cdot}6\,H_2O$, 0.0037; $MnSO_4{\cdot}H_2O$, 0.0016; tryptone, 1.0; Tween-80, 0.15 % (v/v); and 50 mL citrate buffer containing citric acid and

NaOH (pH 4.5)] containing 2 % (w/v) glucose, incubated at 45°C for 36 h. For enzymatic activity, RT-qPCR, and comparative transcriptomic analyses, approximately 5×10^7 fresh spores (final concentration, 1×10^6 spores mL^{-1}) of *M. thermophila* strains were pre-grown in 50 mL Mandels medium containing 2 % (w/v) glucose at 45°C with shaking at 150 rpm for 36 h. Subsequently, mycelia of *M. thermophila* strains were collected and washed with the Mandels medium (without carbon source) and aliquots of wet mycelia (0.55 g) were transferred into 50 mL Mandels medium containing 2 % (w/v) Avicel (Sigma-Aldrich, St. Louis, MO, USA), incubated at 45°C with shaking at 150 rpm for 48–96h. For fungal colony morphology assay, spore suspensions of *M. thermophila* strains (1.5 μL, 1×10^7 mL^{-1}) were dropped onto PDA, solid Mandels medium supplemented with 2 % (w/v) glucose or 1 % (w/v) Avicel as the sole carbon source, and cultivated at 45°C for 3 or 4 days. For growth observation in liquid culture, spores from *M. thermophila* strains were inoculated at a concentration of 1×10^6 spores mL^{-1} in 50 mL Mandels medium with 2 % (w/v) glucose or 2 % (w/v) Avicel and grown at 45°C for 36 h.

Escherichia coli DH5α was used for plasmid construction and propagation, cultivated at 37℃ in ampicillin (100 μg mL^{-1}) supplemented Luria-Bertani (LB) medium.

2.2. Plasmid construction

All primer sequences used in this study are listed in Table S1**.** All PCR products were amplified using Phanta Max Super-Fidelity DNA Polymerase (Vazyme Biotech, Nanjing, China). pFC332, a AMA1 plasmid contains *A. nidulans* optimized Cas9 with attached SV40 nuclear localization signal (PKKKRKV) and hygromycin B resistance gene (*hph*) selection marker, was a gift from Uffe Mortensen (Addgene plasmid # 87845) (Nødvig et al., 2015). The sgRNA (guide RNA) scaffold with the *BsrG*I site was synthesized by IGE Biotechnology (Guangzhou, China) and the double-stranded sgRNA scaffold was gained using the primers sgRNA scaffold-F/R with the aid of annealing buffer for DNA oligos (5 ×) (Beyotime Biotech, Shanghai, China). The U6 promoter of *M. thermophila* was amplified from genomic DNA using the primers U6p-F/R (Liu et al., 2017). The U6 promoter and sgRNA scaffold fragments were cloned into the *Pac*I site of pFC332 via the ClonExpress® Ultra One Step Cloning Kit (Vazyme Biotech, Nanjing, China) to create the plasmid pFC332-Cas9-U6p-sgRNA scaffold following the manufacturer's instructions.

For the disruption of target genes using the CRISPR/Cas9 system, the Cas9-U6p-target gene-sgRNA scaffold expression cassettes were constructed. The protospacer sequences targeting MYCTH_2310243, MYCTH_2302011, MYCTH_2082522, MYCTH_2306976, MYCTH_2297579, MYCTH_2307931, MYCTH_2308823, and MYCTH_2129372, were selected using the sgRNACas9 tool (Xie et al., 2014) with minimized off-target effects. All protospacer sequences that fused with sgRNA scaffold aimed at the eight different genes, and U6 promoters were amplified from pFC332-Cas9-U6p-sgRNA scaffold vector and ligated and cloned into pFC332 vector, which generated the corresponding plasmids Cas9-U6p-*MYCTH_2310243*-sgRNA, Cas9-U6p-*MYCTH_2302011*-sgRNA, Cas9-U6p-*MYCTH_2082522*-sgRNA, Cas9-U6p-*MYCTH_2306976*-sgRNA, Cas9-U6p-*MYCTH_2297579*-sgRNA, Cas9-U6p-*MYCTH_2307931*-sgRNA, Cas9-U6p-*MYCTH_2308823*-sgRNA, and Cas9-U6p-*MYCTH_2129372*-sgRNA. The donor DNA vectors were constructed using selectable maker cassette P*gpd-neo* amplified from plasmid pBC-*neo* (Li et al., 2020c). The 5′ and 3′ flanking fragments of *MYCTH_2310243*, *MYCTH_2302011*, *MYCTH_2082522*, *MYCTH_2306976*, *MYCTH_2297579*, *MYCTH_2307931*, *MYCTH_2308823,* and *MYCTH_2129372* were separately amplified from *M. thermophila* genomic DNA. The resultant 5′, 3′, and P*gpd-neo* fragments were assembled and inserted into pUC19 plasmid digested by *Hin*dIII/*Eco*RI using One Step Cloning Kit (Vazyme Biotech, Nanjing, China) to generate the eight corresponding donor DNA sequences.

For gene overexpression, the strong constitutive promoter of *Mtpdc* (MYCTH_112121, pyruvate decarboxylase), P*gpdA-hph*, and T*tef1* fragment were obtained by separately amplifying from pUC19-P*pdc*-T*pdc* (Wang et al., 2015), PAN7–1(GenBank: Z32698.1), and pFC332 vectors. They were then ligated into the *Hin*dIII and *Eco*RI sites of pUC19 plasmid, generating the plasmid pUC19-P*pdc-hph*. To establish a universal overexpression system in *M. thermophila*, the *MtgpdA* (MYCTH_2311855, glyceraldehyde-3-phosphate dehydrogenase) terminator was amplified from *M. thermophila* gDNA with T*gpdA*-F/T*gpdA*-R primer set. The *Ppdc* and *hph* cassette were amplified in the pUC19-P*pdc-hph* plasmid. The *Ppdc*, *TgpdA,* and *hph* cassette were assembled and inserted into pUC19 plasmid to yield the overexpression plasmid pUC19-P*pdc*-T*gpdA-hph*. The *MYCTH_2307931* overexpressing vector was constructed by amplifying *MYCTH_2307931* using *MYCTH_2307931*-F/R primer set which was then ligated into the *Not*I and *Xba*I sites of universal overexpression pUC19-P*pdc*-T*gpdA-hph* plasmid, creating the pUC19-P*pdc-MYCTH_2307931*-T*gpdA-hph* vector. The One Step Cloning Kit (Vazyme Biotech, Nanjing, China) was utilized to construct MYCTH_2307931-eGFP expression vector (pUC19-P*pdc--MYCTH_2307931-eGFP*-T*gpdA-hph* vector) with enhanced GFP (*eGFP*) fused to *MYCTH_2307931*as a reporter gene.

2.3. Transformation of Myceliophthora thermophila protoplasts

Protoplast preparation and transformation of *M. thermophila* was described in Wang et al. (2015) with the following modifications. For the deletion of genes, approximately 20 μg Cas9-U6p-target genes-sgRNA cassette and 20 μg target genes-donor vector were mixed and added to 200 μL protoplasts suspension of *M. thermophila* wild-type strain. After incubating in protoplast regeneration medium at 30°C for 16 h, the pellet of transformants were maintained in PDA medium contains hygromycin B (75 μg mL^{-1}) and G418(100 μg mL^{-1}) at 45°C for 4–5 days to screen for positive clones. Similarly, for gene overexpression, 20 μg pUC19-P*pdc-MYCTH_2307931*-T*gpdA-hph* vector was transformed into the *M. thermophila* protoplasts and transformants were screened for *hph* resistance with hygromycin B (75 μg mL^{-1}). The pure positive deletion and overexpression transformants were obtained and verified through streaking onto selection plates with corresponding antibiotics for three successive rounds, followed by genomic PCR identification and sequencing with different specific paired primers (Table S1).

2.4. Total DNA and RNA extraction

Total fungal DNA and RNA were extracted from fresh mycelia harvested from respective liquid medium through vacuum filtration. The DNA and RNA were extracted and purified using fungal DNA extraction kit (Sangon Biotech, Shanghai, China) and RNA extraction kit TransZol Up (TransGen Biotech, Beijing, China), respectively, following the manufacturer's protocols. The DNA and RNA were visualized and assessed by electrophoresis and quantified using the NanoDrop 2000 Spectrophotometer (Thermo Scientific, Waltham, MA, USA).

2.5. RNA sequencing and transcriptome analysis

Fresh spores (final concentration, 1×10^6 spores mL^{-1}) of *M. thermophila* WT strain were inoculated into 50 mL Mandels medium with 2 % (w/v) glucose or 2 % (w/v) Avicel as the sole carbon source at 45°C for 36 h. RNA of *M. thermophila* strain cultured on different media were obtained and designated as GRNA (Glucose) and ARNA (Avicel). The *MtFKH1*-specific transcriptomes were analyzed by growing the wild type (WT) and Δ*MtFKH1* strain of *M. thermophila* in Mandels medium supplemented with 2 % (w/v) glucose, and after optimum growth, washed mycelia were transferred into Mandels medium containing 2 % (w/v) Avicel incubated for 48 h followed by RNA extraction. The mRNA was enriched by Oligo (dT) beads and reverse transcribed into cDNA using Illumina NEBNext Ultra RNA Library Prep Kit (New England

Biolabs, Ipswich, MA, USA). The cDNA libraries were constructed and sequenced using Illumina Novaseq6000 by Gene Denovo Biotechnology Co. (Guangzhou, China). The quality reads were mapped against the *M. thermophila* ATCC 42464 genome using HISAT2. v2.4 (Kim et al., 2015). The RSEM software was used to analyze the gene expression levels (fragment per kilobase of transcript per million mapped reads, FPKM) (Li and Dewey, 2011). The differentially expressed genes (DEGs) were identified by DESeq2 (Love et al., 2014), with absolute fold change > 2 ($\log_2$ fold change > 1 or < -1) and adjusted Pvalue (padj) < 0.05 as thresholds. Gene Ontology (GO) enrichment analysis was implemented using the OmicShare tools (https://www.omicshare.com/tools). All DEGs were mapped against GO terms in the Gene Ontology database (http://www.geneontology.org/). Significantly enriched GO terms in DEGs compared with the *M. thermophila* ATCC 42464 genome background were calculated by hypergeometric test. GO terms with Pvalue < 0.05 were considered significantly enriched. The raw reads of transcriptomic data are available at the Gene Expression Omnibus (GEO) under accession number #GSE274481 and #GSE274798.

2.6. Subcellular localization of MYCTH_2307931-GFP in M. thermophila

MYCTH_2307931-GFP positive transformants were inoculated into Mandels medium containing 2 % (w/v) glucose and incubated at 45°C for 36 h. Mycelia were harvested and stained with 5 mg L^{-1} DAPI (4′,6-diamidino-2-phenylindole) solution for 15 min under darkness and then washed with PBS solution three times. Fungal cells were observed using an Olympus BX53 fluorescence microscopy system, with the Olympus cellSens Standard software used for image processing.

2.7. Protein and enzyme activity measurements

Samples of the fermentation cultures (2 mL) from different time points were collected by centrifugation at 4°C, 12,000 rpm for 10 min to remove mycelia and other solid materials. 20 μL unconcentrated culture supernatant was loaded on a 10 % polyacrylamide gel (PAGE Gel Quick Preparation Kit, Yeasen Biotech, Nanjing, China) and ran at 120 V for 80 min in Tris-Glycine-SDS running buffer. The protein bands were stained with Coomassie Brilliant Blue R-250 (Sangon Biotech, Shanghai, China). The concentration of extracellular protein in culture supernatants was determined with a Modified Bradford Protein Assay Kit (Sangon Biotech, Shanghai, China) based on absorbance at 595 nm, using bovine serum albumin (BSA) as the standard. The filter paper cellulase (FPase), endoglucanase (CMCase) and xylanase activities were measured by the method reported previously (Eveleigh et al., 2009; Ma et al., 2016) with some modifications. Briefly, 150, 150, and 100 μL of appropriately diluted crude enzyme solution was added to 600 μL of 50 mM citrate buffer (pH 4.8) containing Whatman No. 1 filter paper (25 mg, 1.0 cm × 3.0 cm; GE Healthcare Limited, Little Chalfont, United Kingdom), 500 μL of 50 mM citrate buffer containing 1 % sodium carboxymethyl cellulose (CMC-Na; Sangon Biotech, Shanghai, China), 100 μL of 50 mM citrate buffer containing 1 % beechwood xylan (Sigma-Aldrich, Darmstadt, Germany), and incubated at 50 °C for 60, 30 and 10 min, respectively. The reducing sugars generated were determined by the 3,5-dinitrosalicylic acid method described earlier (Ghose, 1987) at 540 nm.

The β-glucosidase (pNPGase) and exoglucanase (pNPCase) activities were assayed using *p*-nitrophenyl-β-D-glucopyranoside (pNPG) and *p*-nitrophenyl-β-D-cellobioside (pNPC) (both from Aladdin Biochemical Technology, Shanghai, China) as substrates, respectively, according to the method previously described (Zou et al., 2012; Mansour et al., 2016) with some modifications. In brief, 100 μL of properly diluted culture supernatant was incubated with 100 μL of 1 mg mL^{-1} substrates dissolved in 50 mM citrate buffer (pH 4.8) at 50°C for 30 min. The reaction was terminated by adding 500 μL of 2 % (w/v) Na_2CO_3 and the absorbance was measured at 405 nm on the Synergy™ HTX multi-mode reader (BioTek, winooski, VT, USA). One unit of enzymatic activity (U) was defined as the amount of 1 μmol glucose or *p*-nitrophenol produced by 1 mL enzyme from the substrate per minute under standard assay conditions.

2.8. Real-time quantitative reverse transcription-PCR (RT-qPCR) analysis

The cDNA was synthesized from RNA using HiScript® III RT SuperMix (+gDNA wiper) (Vazyme Biotech, Nanjing, China) following the manufacturer's protocol. Each 20 μL PCR reaction mixture was composed of 10 μL of Hieff UNICON® Universal Blue qPCR SYBR Green Master Mix (Yeasen Biotech, Shanghai, China), 0.4 μL of each primer (10 μM), 2.0 μL of diluted cDNA and 7.2 μL of sterile water. The thermocycler protocol was as follows: initial denaturation for 2 min at 95 °C, followed by 40 cycles of 5 s at 95 °C and 20 s at 63 °C. Melt curves assays were performed after each run to confirm specific amplification of all primers. The primers used for the genes are shown in Table S1. The *actin* gene (*MYCTH_2314852*) of *M. thermophila* was used as an endogenous control and expression levels of the genes were calculated by the comparative CT method $2^{-\Delta\Delta CT}$ (Livak and Schmittgen, 2001). The expression of each tested gene in the WT was set as 100 %. All the experiments were performed in triplicates.

2.9. Expression and purification of the MtFKH1 DNA-binding domain

The DNA fragments encoding the putative DNA-binding domain $MtFKH1_{237–356}$ were amplified from *M. thermophila* genomic DNA. The purified PCR products were inserted into the *Hin*dIII site of pET-51b vector to construct a fusion plasmid pET-51b-$MtFKH1_{237–356}$ and was subsequently introduced into *E. coli* BL21(DE3) for protein expression. The resulting recombinant strain was cultured in LB medium until OD600 was 0.6 and induced with 1.0 mM isopropyl-β-D-thiogalactopyranoside (IPTG) at 28°C for 24 h to produce the Strep II-tagged fusion protein. The recombinant protein was purified using a Strep-Tactin Sepharose High Performance Affinity column (Cytiva, Shanghai, China) according to the supplier's guidelines. The purified protein was verified by sodium dodecyl sulfate-polyacrylamide gel electrophoresis (SDS-PAGE) analysis, and the protein band was excised and identified using LC-MS/MS with PEAKS Studio 8.5 (Bioinformatics Solutions Inc., Waterloo, Canada) analysis system.

2.10. Electrophoretic mobility shift assays

Different DNA fragments were used as probes in the gel-shift assays. For MtFKH1-binding experiments, the promoter regions of *bgl1* (MYCTH_66804) (P1, − 350 to − 1; P2, − 650 to − 300; P3, − 1000 to − 600), *cbh1* (MYCTH_109566) (P1, − 350 to − 1), *xyn1* (MYCTH_112050) (P3, − 1000 to − 650) and *xyr1* (MYCTH_2310145) (P1, − 350 to − 1) were obtained by PCR from the genomic DNA of *M. thermophila* using the primers listed in Table S1. The PCR products were purified using PCR Product Purification Kit (Sangon Biotech, Shanghai, China) and quantified using a NanoDrop 2000 Spectrophotometer (Thermo Scientific, Waltham, MA, USA). The subsequent binding experiments were performed based on a modified gel mobility shift assay reported previously (Wang et al., 2011). In each EMSA reaction, constant amount (100 ng) of the DNA probes were incubated with gradual quantities (0–0.2 μg) of recombinant proteins individually at 25°C for 30 min in solution containing Gel-Shift Binding Buffer (Beyotime Biotech, Shanghai, China). After incubation, the protein-DNA complexes and free DNA were separated by electrophoresis on native 6 % polyacrylamide gels with 0.5 × TBE running buffer (44.5 mM Tris-boric, 1 mM EDTA, pH 8.2) at 110 V for 70 min at 4°C. Finally, gels were visualized with the Bio-Rad Gel-Doc™ Imaging System (Bio-Rad Laboratories Inc., Hercules, CA, USA). Purified Strep II-His-tagged protein from *E. coli* BL21(DE3) cells transformed with the vector pET-51b-$MtCLR\text{-}2_{30–89}$ was used as the negative control.

2.11. DNase I footprinting assays

DNase I footprinting assays were implemented according to a previously reported protocol (Wang et al., 2012). For preparing fluorescent 6-carboxyfluorescein (FAM)-labeled probe, *bgl1* promoter region (P1, −350 to −1) was amplified from *M. thermophila* genomic DNA using the primers *bgl1*-p1-F/R. The FAM-labeled probe was subsequently purified and quantified with NanoDrop 2000 Spectrophotometer. For each assay, 400 ng probe was incubated with various quantities of purified $MtFKH1_{237–356}$ in a total mixture of 40 μL in the same binding buffer as described in EMSAs. After incubation at 25°C for 30 min, 10 μL solution containing 0.015-unit DNase I (Promega, Madison, WI, USA) and 100 nmol $CaCl_2$ were added and further incubated at 25°C for 1 min. The reaction was stopped by adding 140 μL DNase I stop solution (200 mM unbuffered sodium acetate, 30 mM EDTA, and 0.15 % SDS). After enzymatic digestion, the protein was removed by phenol-chloroform extraction, and the DNA was precipitated with ethanol and resuspended in Milli-Q water. The DNA sequencing analysis was performed as previously described (Wang et al., 2012).

3. Results

3.1. Comparative transcriptomic analysis of M. thermophila

Carbon Catabolite Repression (CCR) is a global regulatory system which ensures preferential utilization of glucose or other readily

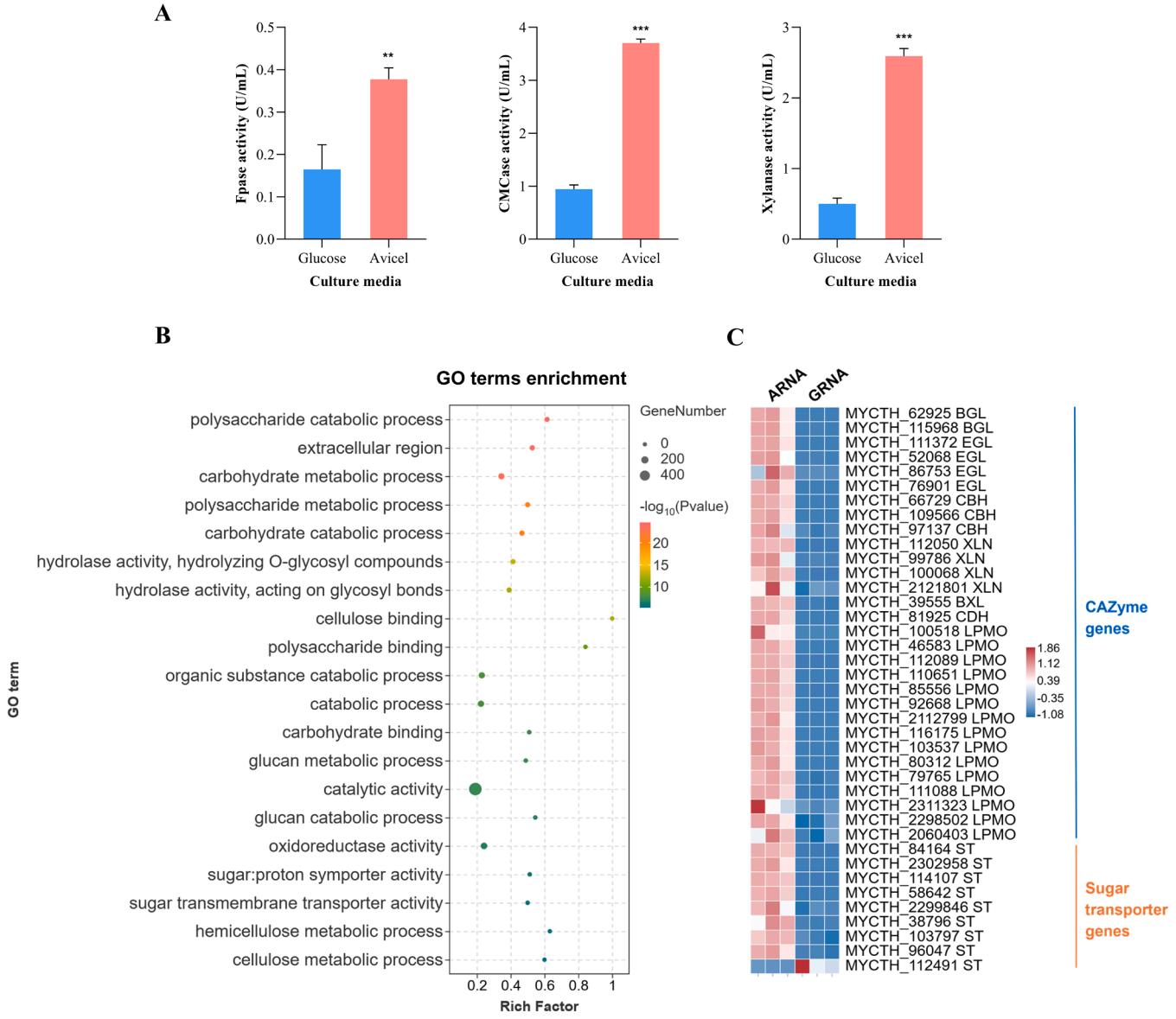

Fig. 1. Comparative transcriptomic analysis of *M. thermophila* grown on Avicel (ARNA) and Glucose (GRNA). **(A)** Enzymatic activities of filter-paper cellulase, endoglucanase, and xylanase of *M. thermophila* cultured for 48 h in 2 % (w/v) Avicel or 2 % (w/v) glucose culture media after a shift from liquid Mandels medium containing 2 % (w/v) glucose. * *$p < 0.01$ and * **$p < 0.001$ indicate significant differences in enzyme activities detected in *M. thermophila* between Avicel and glucose cultures (Student's t tests). Error bars indicate the SD from three replicates. **(B)** Gene Ontology (GO) enrichment analysis of 1558 differentially expressed genes (DEGs) in the Biological Process (BP), Cellular Component (CC), and Molecular Function (MF) categories for *M. thermophila* under Avicel and Glucose conditions. The screening criteria for DEGs are |log2 fold change| > 1 and padj < 0.05. **(C)** Heatmap analysis of expression profiles for the cellulase genes, xylanase genes, xylosidase gene, cellobiose dehydrogenase gene, LPMO (AA9) encoding genes, and putative sugar transporter encoding genes when |log2 fold change| > 2 and padj < 0.05 as thresholds in *M. thermophila* cultured on Avicel compared with that on glucose. BGL, β-glucosidase; EGL, endoglucanase; CBH, cellobiohydrolase; XLN, xylanase; BXL, β-xylosidase; CDH, cellobiose dehydrogenase; LPMO, lytic polysaccharide monooxygenase; ST, sugar transporter.

available carbon sources over less-favored carbohydrates such as cellulose (Adnan et al., 2017; Benocci et al., 2017). Thus, glucose and lignocellulose are the most widely used repressor and inducer for lignocellulolytic enzymes production, respectively. In the current study, the cellulase and xylanase production was evaluated in inducing and repressing carbon sources. As expected, all the enzymatic activities of *M. thermophila*, including filter-paper cellulase (FPase), endo-glucanase (CMCase), and xylanase, increased by 128 %, 292 %, and 417 %, respectively on Avicel compared with that of glucose after 48 h **(**Fig. 1**A)**. Transcription factors (TFs) play a pivotal regulatory role in fugal lignocellulolytic enzymes synthesis. We speculated that TFs may be responsible for the improvements in cellulase and xylanase activities observed under Avicel conditions. Therefore, the transcriptomes of *M. thermophila* wild type (WT) cultured on Avicel and glucose were screened for potential regulators of cellulolytic and xylanolytic genes expression.

The total RNAs obtained from the mycelia of *M. thermophila* grown on Aviel or glucose for 36 h were sequenced. There were 24–34 million quality reads generated > 92 % were mapped onto the *M. thermophila* genome (Table S2).

Compared to glucose as the carbon source, 1558 differentially expressed genes (DEGs) were identified in *M. thermophila* when grown in Avicel, comprising 752 upregulated and 806 downregulated genes (Table S3). Gene Ontology (GO) enrichment analysis revealed that these DEGs were enriched in polysaccharide catabolic process, carbohydrate metabolic process, and polysaccharide metabolic process (Biological Process) or hydrolase activity acting on glycosyl bonds, and cellulose or polysaccharide binding (Molecular Function) (Fig. 1**B** and Table S4).

The comparative transcriptome analysis also uncovered substantial differences in the expression of 10 genes encoding putative transcription factors when |log2 fold change | > 2 and padj < 0.05 were used as thresholds, of which, four genes were upregulated and six were downregulated when cultivated on Avicel (Table 1). Based on the DNA-binding domain or transcriptional activation domain predicted by bioinformatics, these TFs were classified into seven types: High Mobility Group (HMG), Helix-loop-helix (HLH), Fungal_TF, Zinc finger (Zn2Cys6, C2H2), Forkhead, basic-leucine zipper (bZIP), and CP2 transcription factor (Table 1). It is noteworthy that MYCTH_38704 (MtCLR-2) and MYCTH_2310995 (MtHAC-1) were found to regulate cellulase secretion in *M. thermophila* (Li et al., 2022; Zhang et al., 2022).

Furthermore, nine key cellulase genes including two β-glucosidase genes *MYCTH_62925* and *MYCTH_115968*, four endoglucanase genes (*MYCTH_111372*, *MYCTH_52068*, *MYCTH_86753*, and *MYCTH_76901*), and three cellobiohydrolase genes (*MYCTH_66729*, *MYCTH_109566*, and *MYCTH_97137*), five crucial xylanolytic genes including four crucial xylanase genes (*MYCTH_112050*, *MYCTH_99786*, *MYCTH_100068*, and *MYCTH_2121801*), and a xylosidase gene *MYCTH_39555*, were substantially upregulated on Avicel relative to those on glucose (Fig. 1**C**), demonstrating that considerably improved lignocellulolytic enzyme activities detected in cellulose culture (Fig. 1**A**).

Additionally, 15 LPMOs (AA9) encoding genes were strongly induced on Avicel cultivation (Fig. 1**C**). Lytic polysaccharide monooxygenases (LPMOs) are copper-dependent enzymes that split glycosidic linkages on the surface of cellulose in an oxidative manner, thus promoting cellulase access to the glycosidic bonds within the polysaccharides (Kjaergaard et al., 2014). Moreover, a gene encoding cellobiose dehydrogenase gene (*MYCTH_81925*, MtCDH-2), which is deemed the primary redox partner of LPMOs being expressed and secreted in the presence of cellulose (Phillips et al., 2011), was also upregulated by the presence of Avicel (Fig. 1**C**).

In addition to these CAZyme genes, eight putative sugar transporter encoding genes including *MYCTH_84164* (cellodextrin transporter-like protein1, CLp1 ortholog) (Cai et al., 2015), *MYCTH_2302958* (ortholog of CLp1), *MYCTH_114107* (cellodextrin transport-2, CDT-2 ortholog) (Znameroski et al., 2014), *MYCTH_58642*, *MYCTH_2299846*, *MYCTH_38796*, *MYCTH_103797*, and *MYCTH_96047* were highly induced in *M. thermophila* strain during growth in Avicel, except for *MYCTH_112491* (Fig. 1**C**). These observations were consistent with the findings that numerous sugar transporter-encoding genes were upregulated in the presence of sugarcane bagasse or wheat straw but repressed by glucose (de Souza et al., 2011; Ries et al., 2013), suggesting that these genes were required for better utilization of diverse sugars generated form complex biomass degradation.

Expression pattern analyses also identified a few genes linked to carbon metabolism pathways. With regards to gluconeogenesis, one upregulated and three downregulated genes were detected when cells were grown in Avicel. The DEGs included triosephosphate isomerase gene *MYCTH_2304931*, fructose-bisphosphatase gene *MYCTH_2306943*, phosphoenolpyruvate synthase gene *MYCTH_2311072*, and phosphoenolpyruvate carboxykinase gene *MYCTH_2315623*. Similarly, four genes involved in the tricarboxylic acid (TCA) cycle were characterized, including one upregulated (succinyl-CoA ligase *MYCTH_2296474*), and three downregulated genes (isocitrate lyase *MYCTH_110871*, aconitate hydratase *MYCTH_2309261*, and 2-oxoglutarate dehydrogenase *MYCTH_2312383*) on Avicel compared with those on glucose. The varied expression of these genes involved in anabolic and catabolic metabolism may be beneficial to efficient utilization of cellulose as the carbon source under carbon starvation conditions.

Table 1
Candidate TFs from transcriptomic analysis of *M. thermophila* on Avicel and glucose.

Gene symbol	InterPro annotation[a]	Domain description	Log2FoldChange[b]
MYCTH_2129372	IPR009071	High Mobility Group (HMG)-box	7.22
MYCTH_2310243	IPR011598	Helix-loop-helix (HLH)	4.86
MYCTH_38704	IPR007219	Fungal_TF	3.62
MYCTH_2308823	IPR001138	Zinc finger, Zn2Cys6	2.11
MYCTH_2306976	IPR001138	Zinc finger, Zn2Cys6	−7.04
MYCTH_2307931	IPR001766	Forkhead domain	−4.25
MYCTH_2310995	IPR004827	basic-leucine zipper (bZIP)	−2.69
MYCTH_2297579	IPR013087	Zinc finger, C2H2	−2.20
MYCTH_2082522	IPR007604	CP2 transcription factor	−2.12
MYCTH_2302011	IPR001138	Zinc finger, Zn2Cys6	−2.06

[a] (https://www.ebi.ac.uk/interpro/)
[b] Gene expression levels of *M. thermophila* cultivated on Avicel compared to glucose.

3.2. Novel regulatory gene potentially regulating cellulase and xylanase production

To identify novel TFs controlling cellulase and xylanase production in *M. thermophila*, a CRISPR/Cas9 system was established to create deletion strains of eight potential regulatory genes (Fig. S1A**-B**). Protospacer sequences containing 20-nucleotide targets for the eight candidate genes were designed for gene editing (Table 2). The resultant disruption mutants were confirmed by PCR using three specific primer sets (Table S1), and five candidate genes were successfully deleted (Fig. S1C**-D**). Measurements of enzymatic activities in the deletion mutants (Δ*MYCTH_2310243*, Δ*MYCTH_2306976*, Δ*MYCTH_2307931*, Δ*MYCTH_2308823*, and Δ*MYCTH_2129372*) compared with WT under Avicel conditions revealed that Δ*MYCTH_2307931* showed 31 % and 34 % enhancement in Fpase and xylanase activity, respectively (Fig. S1E). Hence, the TF encoding gene *MYCTH_2307931* was considered for all downstream analysis.

3.3. MYCTH_2307931 acts as a forkhead transcription factor

The *MYCTH_2307931* gene contains two exons encoding a 724 amino acids (aa) protein. The InterPro analysis (https://www.ebi.ac.uk/interpro/) showed the presence of a forkhead DNA-binding domain

Table 2
List of protospacer and protospacer adjacent motif (PAM) sequences of each target gene used in this study.

Gene symbol	Protospacer sequence	PAM
MYCTH_2129372	TTCTGCGAGGCACATGCGCC	CGG
MYCTH_2310243	TCTCACGGTCCATTAGTCGA	TGG
MYCTH_2308823	GCGCTACGATGCACAACACC	GGG
MYCTH_2306976	TATGGGCGCCTGACTGTTCA	AGG
MYCTH_2307931	CTGTGCCTCTCCTGCACAAC	AGG
MYCTH_2297579	GTCGCAACGCACTATGCGCC	TGG
MYCTH_2082522	GCTACTATACGCCCACTTCG	GGG
MYCTH_2302011	CAATGACGTTCCCGTTCCAG	AGG

(IPR001766) between the residue positions 237 and 356 (Fig. 2). Additionally, protein alignment using BLASTP indicated that MYCTH_2307931 shares 28–44 % identity with its close homologs from different organisms including *S. cerevisiae* (ScFKH1, GenBank: DAA08422.1; ScFKH2, GenBank: DAA10477.1), *H. chrysogena* (HcFKH1, GenBank: AAP35674.1), *A. nidulans* (AnFKHB, GenBank: CBF83869.1), and *P. oxalicum* (PoX08522, GenBank: AOP12492.1) with high similarity confined in the DNA-binding forkhead domain (Fig. 2). All matching proteins have been characterized as members of the forkhead TFs family with diverse roles in microbial development and metabolism. MYCTH_2307931 is subsequently re-designated as MtFKH1 (where Mt represents *M. thermophila* and FKH represents forkhead) since it is the first forkhead protein functionally characterized in *M. thermophila*.

3.4. MtFKH1 plays a key role in cellulase and xylanase production

To further explore the regulatory roles of *Mtfkh1*, *M. thermophila* Δ*Mtfkh1* strain and the WT parental strain were cultivated in liquid Mandels medium containing 2 % (w/v) Avicel for 48–96h after a shift from glucose with equal amount of starting inoculum (0.55 g). The results revealed that cellulase activities corresponding to FPase, pNPCase, and pNPGase activities, as well as xylanase production of Δ*Mtfkh1* were increased by 25–42 %, 36–57 %, 31–62 %, and 34–86 % respectively, compared with the WT (Fig. 3**A-D**). Additionally, Δ*Mtfkh1* secreted approximately 141–158 % higher protein than the WT when grown on Avicel (Fig. 3**E**). These results were validated by the SDS-PAGE analysis of the extracellular protein (Fig. 3**F**).

To further verify the alterations in cellulase and xylanase production in the mutant Δ*Mtfkh1* caused by the specific disruption of the *Mtfkh1* gene, the overexpression strain OE-*Mtfkh1* was generated, in which *Mtfkh1* was driven by a strong constitutive promoter P*pdc* (MYCTH_112121, pyruvate decarboxylase). The positive overexpression mutant was confirmed by PCR with specific primers (Table S1 and Fig. S1). Evaluation of the enzyme production showed a 26–55 % decrease in FPase, pNPCase, pNPGase, and xylanase yields, as well as extracellular protein content, by OE-*Mtfkh1* strain, during the presence of Avicel relative to the activities detected in the WT (Fig. 3**A-E**). These findings indicate that MtFKH1 is a repressor of cellulase and xylanase production.

3.5. MtFKH1 controls sporulation in M. thermophila

To evaluate the role of MtFKH1 in growth phenotype, *M. thermophila* WT, Δ*Mtfkh1*, and OE-*Mtfkh1* strains were cultivated on solid plates containing glucose or Avicel as the sole carbon source, and PDA plates. None of these *M. thermophila* strains displayed considerable differences in colony phenotype on all tested culture media (Fig. 4**A**). The quantitative assessment of the asexual spores produced by strains WT, Δ*Mtfkh1*, and OE-*Mtfkh1* on Avicel plates was also carried out. Surprisingly, Δ*Mtfkh1* produced only 38 % of the spores generated from the WT after 7 days, whereas OE-*Mtfkh1* presented similar level of conidia formation with the WT (Fig. 4**B**). The hyphal growth observed in Δ*Mtfkh1* mutant incubated in liquid shake flasks containing glucose or Avicel as the sole carbon source was consistent with its growth on glucose or cellulose solid plates, exhibiting no noticeable differences relative to that detected in both WT and OE-*Mtfkh1* strains (Fig. 4C and Fig. S2), which was also confirmed by microscopic investigation (Fig. S2). Taken together, these results suggest that MtFKH1 regulates sporulation not fungal growth.

3.6. Subcellular localization of MtFKH1 in M. thermophila

To determine whether MtFKH1is a nuclear protein, the *Mtfkh1* encoding gene was fused to a *gfp* (green fluorescent protein) gene under the control of the powerful constitutive promoter P*pdc*. The expression vector was introduced to the WT strain to generate the overexpression strain expressing the MtFKH1-GFP fusion protein. The green

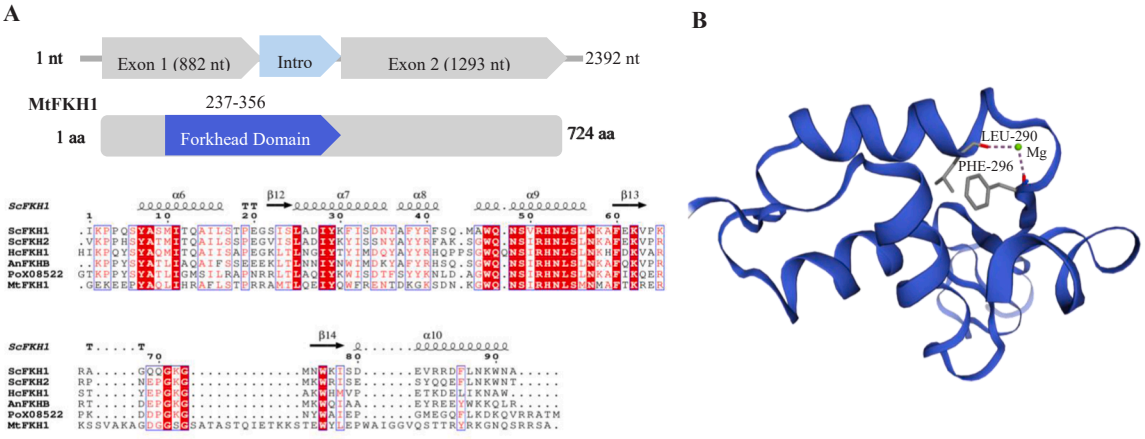

Fig. 2. Characterisation of the MYCTH_2307931 as a forkhead protein. **(A)** Analysis of conserved domain in the MtFKH1 protein and protein sequence alignment. The MtFKH1 gene possesses two exons, and the predicted Forkhead DNA-binding domain (DBD) is highlighted. Protein alignment of the DBD between MtFKH1 and previously reported forkhead proteins in *Saccharomyces cerevisiae* S288C (ScFKH1, GenBank: DAA08422.1; ScFKH2, GenBank: DAA10477.1), *Hapsidospora chrysogena* (HcFKH1, GenBank: AAP35674.1), *Aspergillus nidulans* FGSC A4 (AnFKHB, GenBank: CBF83869.1), and *Penicillium oxalicum* HP7–1 (PoX08522, GenBank: AOP12492.1) confirmed the presence of conserved amino acids (aa) within the DBD. The identical aa are highlighted in red boxes, and aa in red characters with blue frames indicate similar amino acid residues across different proteins. α, β, and TT represent α-helices, β-strands, and β-turns, respectively, in DBD of ScFKH1, which was obtained from SWISS-MODEL (P40466). **(B)** The tertiary structure of the DBD of MtFKH1 was gained by homology modelling using SWISS-MODEL. The green ball represents magnesium ion.

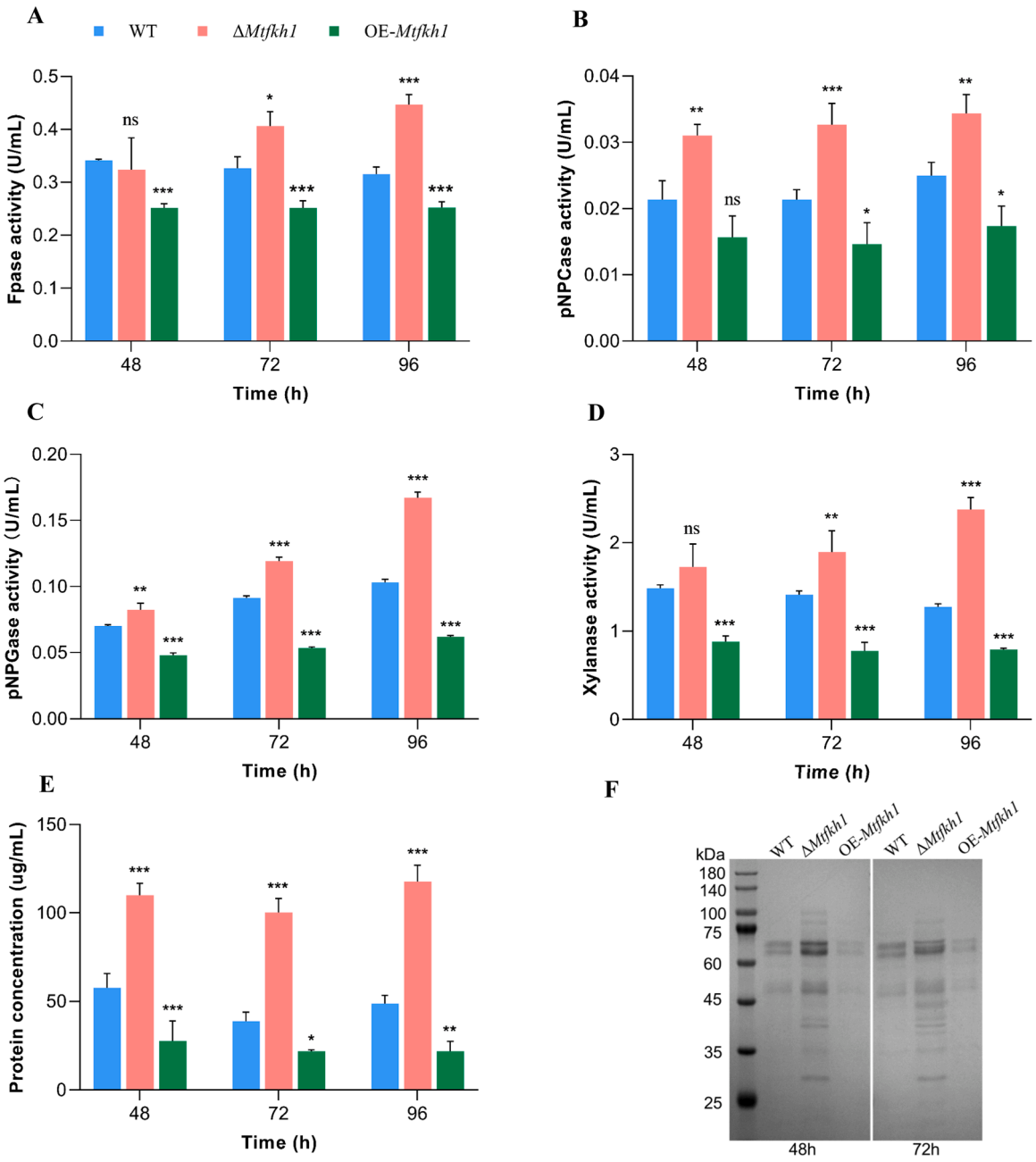

Fig. 3. Enzyme activities and protein production of *M. thermophila* WT strain, ΔMtfkh1 deletion mutant, and OE-Mtfkh1 overexpression strain. Culture supernatants were collected from fungal strains cultivated on Avicel for 48–96h at 45°C after shifting from glucose. **(A)** Filter paper cellulase (FPase) activity. **(B)** Cellobiohydrolase (pNPCase) activity. **(C)** β-glucosidase (pNPGase) activity. **(D)** Xylanase activity. **(E)** Extracellular protein concentration. **(F)** SDS-PAGE analysis of the secreted proteins at 48 and 72 h. M, 10–180 kDa protein marker. *$p < 0.05$, * *$p < 0.01$, and * **$p < 0.001$ indicate remarkable differences in enzyme activities and secreted protein detected between WT and ΔMtfkh1 or OE-Mtfkh1 strains (Two-way ANOVA), ns indicates not significant. Error bars represent the SD from three replicates.

fluorescence signal was observed in the intracellular nuclei across the fungal cells, which merged well with the nucleic acid-specific blue dye DAPI (Fig. 4**D**), demonstrating that MtFKH1 is located in the *M. thermophila* nucleus.

3.7. MtFKH1 regulates the expression of major cellulase and xylanase genes

To investigate whether MtFKH1 transcriptionally controls the expression of cellulase and xylanase genes in *M. thermophila* grown on cellulose, real-time quantitative reverse transcription PCR (RT-qPCR) was performed, with the WT as the control. The transcription levels of key cellulase and xylanase genes as well as genes encoding two crucial regulators Cre1 and Xyr1 in *M. thermophila*, including β-glucosidase gene *bgl1*(*MYCTH_66804*), cellobiohydrolase gene *cbh1* (*MYCTH_109566*), xylanase gene *xyn1* (*MYCTH_*112050), *cre1* (*MYCTH_2310085*), and *xyr1* (*MYCTH_2310145*) were measured at 48 and 72 h after transferring from glucose to Avicel. The results indicated that *cbh1* showed 1.6- and 6.6-fold enhancements in transcription levels in Δ*Mtfkh1* at 48 and 72 h, respectively. Likewise, *bgl1* exhibited 1.0-fold elevation in transcript level at 48 h and slight increase (62 %) at 72 h due to the deletion of *Mtfkh1* in *M. thermophila*. In addition, the expression of *xyn1* in Δ*Mtfkh1* was increased by 63–94 % during the overall period, whereas no change was observed in the transcript levels of *cre1* and *xyr1* at both 48 and 72 h (Fig. 5). These data suggest that the expression of the major cellulase and xylanase genes was significantly improved in Δ*Mtfkh1* compared with

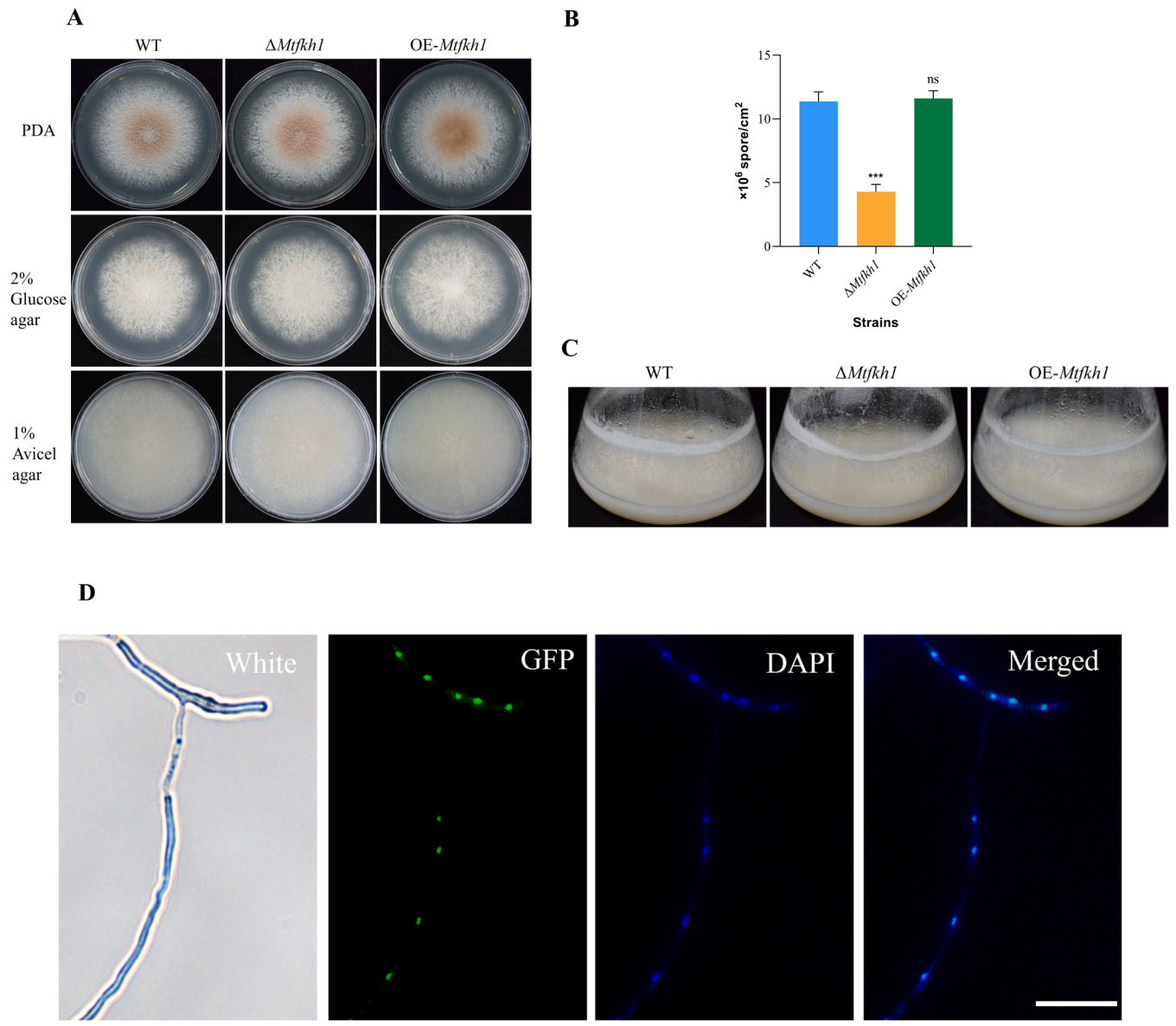

Fig. 4. Phenotypic analyses of *M. thermophila* WT, ΔMtfkh1 and OE-Mtfkh1 strains, and subcellular localization of MtFKH1 protein. **(A)** Colony phenotype on PDA, solid plates containing 2 % (w/v) glucose or 1 % (w/v) Avicel as the sole carbon source after 3 (PDA) or 4 days (glucose and Avicel) of growth at 45°C. **(B)** Quantitative evaluation of conidiation on plates containing 1 % (w/v) Avicel incubated at 45°C for 7 days. * $**p < 0.001$ demonstrates significant differences in sporulation between WT and ΔMtfkh1 strains (Student's t tests), ns represents no remarkable differences between WT and OE-Mtfkh1 strains. Error bars indicate the SD from three replicates. **(C)** Growth observation in liquid shake cultures containing 2 % (w/v) Avicel grown at 45°C for 36 h. **(D)** Subcellular location of MtFKH1 in *M. thermophila*. MtFKH1-GFP strain was grown in liquid Mandels medium with 2 % (w/v) glucose as sole carbon source at 45°C for 36 h. Location of MtFKH1 was monitored by merging EGFP signal and blue florescence signal which was from nuclei-specific dye DAPI. Samples were observed using an Olympus BX53 fluorescence microscope. Scale bar = 20 μm.

WT at certain periods during the presence of Avicel, although with varied degrees.

3.8. *MtFKH1 binds to the promoter regions of crucial cellulase and xylanase genes*

The above findings revealed that MtFKH1 regulates cellulase and xylanase production in *M. thermophila* by controlling transcript levels of cellulolytic and xylanolytic genes. To confirm whether MtFKH1 directly regulates targeted genes expression, electrophoretic mobility shift assays (EMSAs) were performed. Strep II-fused DNA binding domain of MtFKH1 ($MtFKH1_{237–356}$) was expressed and purified from *E. coli* BL21 (DE3) (Fig. S3). Probes covering the promoter regions of *bgl1*(− 1 to − 1000), *cbh1*(− 350 to − 1), *xyn1*(− 1000 to − 650), and *xyr1*(− 350 to − 1) were amplified by PCR. Increased binding was observed for promoter regions of both *bgl1*, *cbh1*, and *xyn1* with different amount of the recombinant $MtFKH1_{237–356}$, and the size of each shifted band increased along with increasing quantity of $MtFKH1_{237–356}$ (0–0.2 μg) (Fig. 6). In contrast, no retardation was detected between $MtFKH1_{237–356}$ and the *xyr1* promoter, which was used as the negative control. Additionally, purified Strep II-fused $MtCLR\text{-}2_{30–89}$ was also utilized as a negative control to exclude the possibility that Strep II-His tag protein bound to the target genes (Data not shown). Taken together, the EMSAs results indicate that MtFKH1 specifically binds to the promoter regions of key cellulase and xylanase genes *bgl1*, *cbh1*, and *xyn1in vitro*.

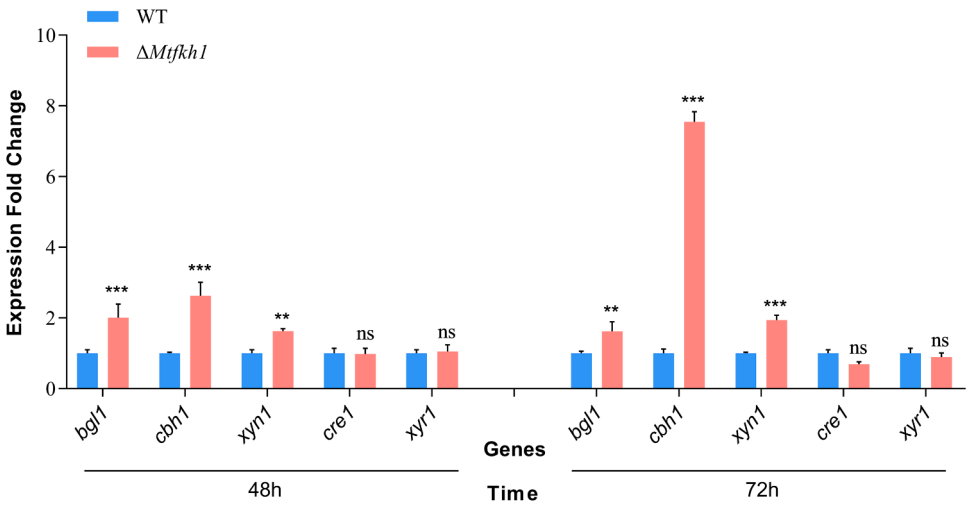

Fig. 5. Relative transcription levels of genes associated with lignocellulose degradation in *M. thermophila* WT and ΔMtfkh1 strains. Strains were pre-cultured in glucose for 36 h, washed and shifted to 2 % (w/v) Avicel medium and cultivated for 48 and 72 h. Expression levels of the detected genes in ΔMtfkh1 were normalized against WT. Asterisks on bars represent notable differences from unmarked bars in each group (Two-way ANOVA, $^{**}p < 0.01$, and $^{***}p < 0.001$), ns indicate no remarkable differences. Error bars represent the SD from three replicates.

3.9. Identification of MtFKH1 binding sites in the upstream region of Mtbgl1

To confirm the precise DNA region bound by MtFKH1 in the promoter of *bgl1*, a DNase I footprinting assay was performed using purified MtFKH1$_{237–356}$ and the FAM-labeled promoter fragment of *bgl1*(P1, − 350 to − 1), which exhibited the strongest specific shift (Fig. 6). As the abundance of MtFKH1 protein increased to 2 μg, one apparently protected region was observed in *bgl1*-P1(5′-CGGGAAGGCAAACATTGT-3′) (Fig. 7**A**), matching the consensus 5′-G/A T/C C/A A A T/C A-3′ (underlined) characterized from 17 different promoter sequences bound by other various forkhead proteins (Kaufmann et al., 1995). It was speculated that 5′-RYMAAYA-3′ might be a conserved motif that MtFKH1 binds to in *M. thermophila*. Therefore, the binding site in the *bgl1*-p2, *bgl1*-p3, *cbh1*-p1, and *xyn1*-p3 were tested. The results identified at least one similar motif in the upstream region of each target gene (5′-RYMANYA-3′), with the "ANYA" sequence highly conserved (Fig. 7**B**). As expected, no 5′-RYMANYA-3′ site was found in *xyr1*-p1.

3.10. Transcriptome analysis of the Mtfkh1 deletion mutant

To comprehensively characterize the regulation of MtFKH1, transcriptional profiling analysis of the WT and Δ*Mtfkh1* strains cultured on Avicel for 48 h after transferring from glucose was conducted. Compared to the WT strain, Δ*Mtfkh1* displayed significantly changed transcription levels of 734 genes, with 221 genes being substantially upregulated and 513 genes being substantially downregulated (Table S5). The GO analysis of the DEGs in Δ*Mtfkh1* showed that hydrolase activity (acting on glycosyl bonds), polysaccharide binding, and carbohydrate metabolic process were highly enriched functional categories (Fig. 8**A** and Table S6), which was in accordance with the phenotypes detected in Δ*Mtfkh1* during the presence of cellulose. Comparative transcriptomic analysis revealed that 17 CAZyme-encoding genes exhibited altered transcription levels in Δ*Mtfkh1* (Fig. 8**B**), among which, two cellobiohydrolase genes including *cbh1* (*MYCTH_109566*) and *MYCTH_66729* were upregulated in Δ*Mtfkh1* compared with WT strain, which could explain the enhanced cellobiohydrolase activity in *Mtfkh1* deletion mutant. However, *MYCTH_42937* and *MYCTH_51545*, which also encode cellobiohydrolase, were downregulated in Δ*Mtfkh1*, indicating that the two cellobiohydrolase encoding genes might contribute less to the secreted enzyme. Similarly, the high expression of the three xylanase genes (*MYCTH_100068*, *MYCTH_52904*, *MYCTH_49824*) and low transcription of xylanase gene *MYCTH_99786* could be responsible for the improved xylanase

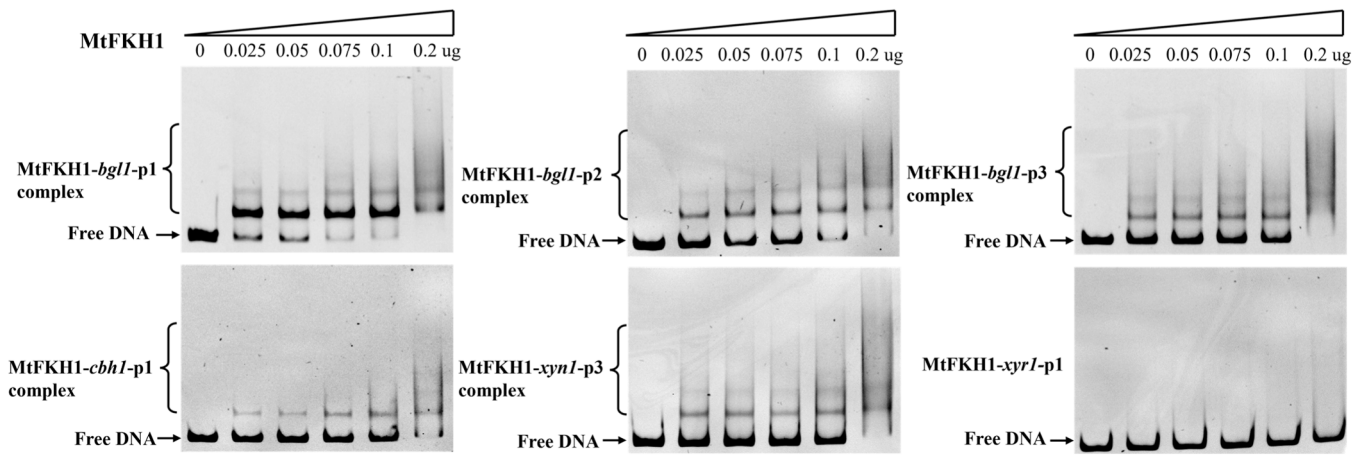

Fig. 6. Electrophoretic mobility shift (EMSA) analysis of the interactions between MtFKH1 and the promoter regions of key genes encoding cellulase and xylanase. Each experiment contains 100 ng probe and indicated quantities of purified MtFKH1 binding domain. The promoter of *xyr1* was used as negative control.

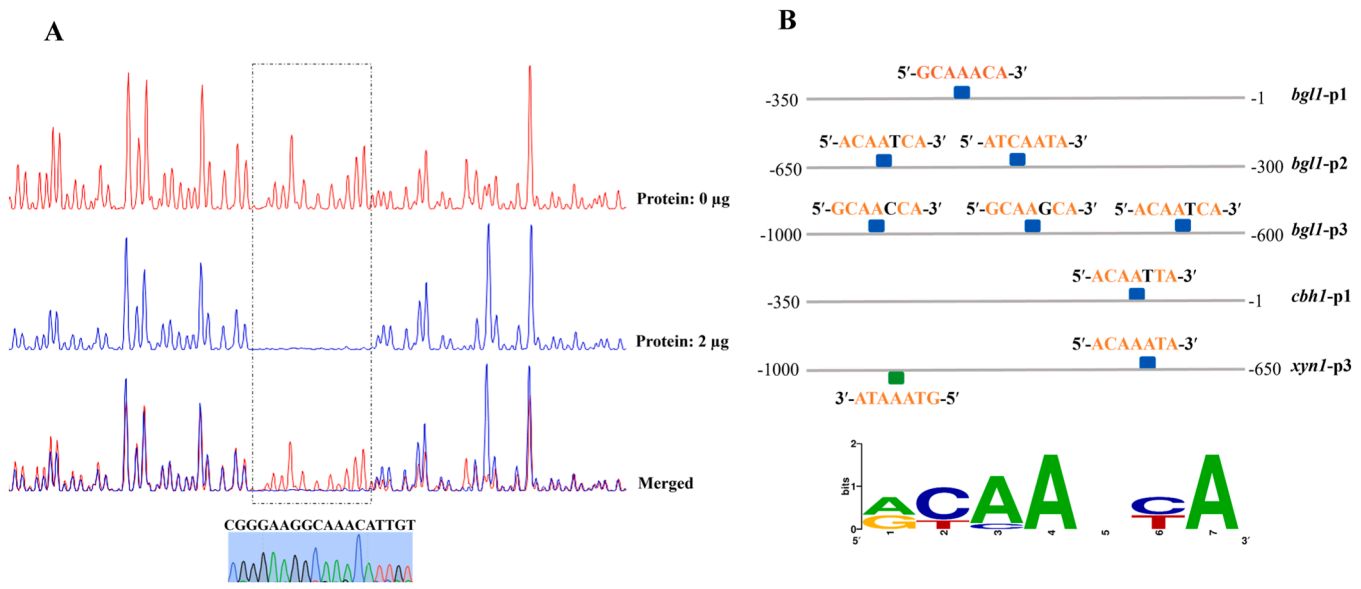

Fig. 7. Identification of the sequence bound by MtFKH1 in the promoter regions of crucial cellulase and xylanase genes. **(A)** Identification of the MtFKH1-protected sequence in the *bgl1* upstream region (*bgl1*-P1) by performing DNase I footprinting assay. The upper two-colored lines indicate the different amounts of MtFKH1 used: red, 0 μg; blue, 2 μg. The merged red and blue lines identify the DNA sequence protected from DNase I degradation, which is presented in dashed box. **(B)** Schematic diagram of the putatively conserved MtFKH1 binding motif in the promoter regions of *bgl1*, *cbh1*, and *xyn1*. Nucleotides in orange represent the identical, whereas that in black indicate the altered compared to the consensus 5′-RYMAAYA-3′. blue box, sense strand; green box, antisense strand.

production observed in Δ*Mtfkh1*. Moreover, three LPMO (AA9) encoding genes (*MYCTH_80312*, *MYCTH_46583*, and *MYCTH_100518*) showed higher transcript levels in Δ*Mtfkh1* than in the WT strain.

Besides CAZyme genes, expression levels of genes encoding putative transcription factors were also altered, with four genes being increased and fourteen genes being decreased in Δ*Mtfkh1*, the majority of which belong to Fungal Zn(II)2Cys6 and Zinc finger (C2H2) families (Fig. 8**C**). All these TF-encoding genes are unidentified except for *MYCTH_2301920*, encoding an essential regulator AmyR for starch utilization in *M. thermophila*, overexpression of which exhibited 30 % elevation in amylase activity (Xu et al., 2018).

Seven genes encoding sugar transporters were also observed showing increased expression levels in Δ*Mtfkh1* relative to WT (Fig. 8**D**). Among them, *MYCTH_2308157* and *MYCTH_112491* encode orthologs of high-affinity (HGT-1) and low-affinity glucose transporter (GLT-1), respectively (Wang et al., 2017). In *N. crassa*, individual deletion of *hgt-1* or *glt-1* showed less effect on cellulase expression (Wang et al., 2017). In contrast, a putative cellodextrin transporter protein CLP1-encoding gene *MYCTH_2302958* was downregulated in Δ*Mtfkh1*. CLP1 represses cellulase induction on both cellobiose and Avicel in *N. crassa*, although it cannot transport cellodextrin (Cai et al., 2015), suggesting that MtCLP1 might also affect cellulase induction pathway.

4. Discussion

In the present study, a novel transcription factor (MtFKH1) that negatively regulates cellulase and xylanase genes expression in *M. thermophila* was functionally characterized via comparative transcriptome and genetic analyses. These two approaches are regarded as highly-efficient approaches in screening novel TFs, as described in the characterization of regulators HCR-1 in *N. crassa* (Li et al., 2014), PoxMBF1 in *P. oxalicum* (Zhao et al., 2019), TpRfx1 in *Talaromyces pinophilus* (Liao et al., 2018), and ACE4 in *T. reesei* (Chen et al., 2021). *M. thermophila* is a thermophilic fungus with huge potential for application in the conversion of plant biomass in biorefineries (Visser et al., 2011; Gu et al., 2023). In this study, transcriptional profiling was implemented on *M. thermophila* grown under different conditions (Avicel and glucose), and transcript levels of genes encoding transcription factors, CAZymes, sugar transporters and those involved in gluconeogenesis and TCA cycle were found to vary. Many CAZyme genes, including key cellulase, xylanase, and LPMO (AA9) genes, were highly induced by Avicel, indicating complex synergy between various enzymes involved in lignocellulose degradation. Specifically, eight novel candidate TFs showed different transcription levels between Avicel and glucose media and five of them were successfully deleted by the newly established CRISPR/Cas9 system, which led to the identification of a forkhead TF. Notably, the deletion of this nuclear localized transcription factor MtFKH1 dramatically increased cellulase and xylanase production, whereas the overexpression of MtFKH1 decreased cellulase and xylanase secretion under Avicel induction. This suggests that MtFKH1 is a repressor of cellulase and xylanase biosynthesis. Intriguingly, the endoglucanase activity was unaffected by the disruption of *Mtfkh1* (Fig. S4), consistent with the expression level of the major endoglucanase genes. The transcription of three endoglucanase genes (*MYCTH_76901*, *MYCTH_116157* and *MYCTH_86753*) was elevated in Δ*Mtfkh1* compared to WT, whereas *MYCTH_52068*, that also encodes endoglucanase, was reduced, implying a self-equilibrating mechanism that tunes biosynthesis of cellulase. Overall, this study provides a candidate target for fungal strain engineering to enhance cellulase and xylanase yields.

The forkhead regulator has been shown to participate in the regulation of cellulase and xylanase gene expression. In *P. oxalicum*, Δ*Pox08522* mutant showed an 81 % increase in the xylanase activity but with a 72 % decrease in β-glucosidase activity compared with the parent strain (Zhao et al., 2016). In this study, the regulatory roles of the forkhead proteins in cellulase and xylanase production in the filamentous fungus *M. thermophila* was further explained. Compared with the forkhead regulator Pox08522, the loss of *Mtfkh1* resulted in an enhancement in both cellulase and xylanase production, indicating the overlapping and divergent functions of forkhead regulators involved in lignocellulose degradation. Comparative transcriptomic analysis showed the pronounced upregulated expression of the cellobiohydrolase and xylanase genes in the Δ*Mtfkh1* mutant when cultivated in Avicel. Conversely, *cre1* and *xyr1*, which encode the major regulator of cellulase and/or xylanase, expressed no significant differences between the Δ*Mtfkh1* mutant and the WT strain, which was also confirmed by the

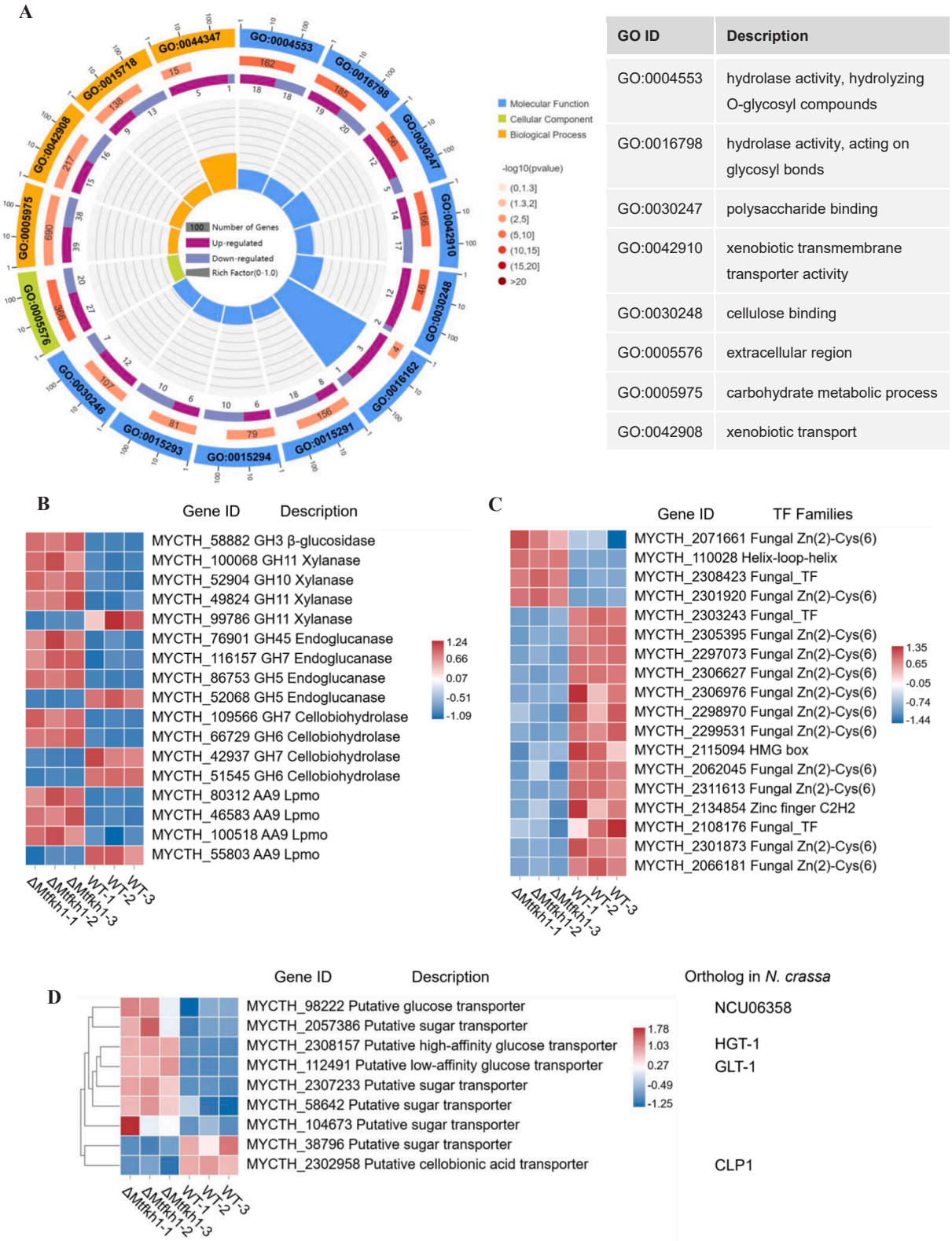

GO ID	Description
GO:0004553	hydrolase activity, hydrolyzing O-glycosyl compounds
GO:0016798	hydrolase activity, acting on glycosyl bonds
GO:0030247	polysaccharide binding
GO:0042910	xenobiotic transmembrane transporter activity
GO:0030248	cellulose binding
GO:0005576	extracellular region
GO:0005975	carbohydrate metabolic process
GO:0042908	xenobiotic transport

Fig. 8. Transcriptional profiling analysis between WT and Δ*Mtfkh1* cultivated on Avicel for 48 h after a shift from glucose. **(A)** Functional enrichment of 734 DEGs in Δ*Mtfkh1* strain within the Molecular Function (MF), Cellular Component (CC), and Biological Process (BP) categories in GO analysis. The left circle diagram represents GO enrichment, from periphery to inner circle, the first circle, ID of GO term; the second circle, the number of genes of specific GO term in *M. thermophila* genome background, and p value; the third circle, the number of upregulated and downregulated genes of the given GO term in Δ*Mtfkh1* compared to that in WT strain; the innermost layer, rich factor, which corresponds of the proportion of DEGs in all background genes in a specific GO term. The right table lists the major enriched GO terms and corresponding descriptions. **(B-D)** Heatmap analysis of transcript levels for genes encoding CAZymes, putative TFs, and putative sugar transporters, respectively, between Δ*Mtfkh1* and WT during the presence of Avicel.

RT-qPCR assay. Of note, the expression of β-glucosidase gene *bgl1* (*MYCTH_66804*) exhibited a 62 %-100 % increase in expression in Δ*Mtfkh1* compared to WT according to RT-qPCR analysis. This observation was seen in the transcriptomic data, demonstrating a 41 % elevation (log2 fold change = 0.5), although not statistical significant. Comparative transcriptome profiling revealed upregulation of *bgl3* (*MYCTH_58882*), another gene encoding β-glucosidase, in the Δ*Mtfkh1* mutant.

In addition, several sugar transporter-encoding genes exhibited altered expression levels (seven upregulated and two downregulated) in Δ*Mtfkh1*. In fungi, sugar transporters are closely associated with nutrient uptake and sense of molecular signals to suppress or activate lignocellulolytic enzyme induction, such as CDT-1/2 and CLP1 in *N. crassa* (Znameroski et al., 2014; Cai et al., 2015), and arabinose transporter MtLat-1 from *M. thermophila* (Gu et al., 2023). Whether the changed transcript levels of these sugar transporters are responsible for the high cellulase and xylanase activities in Δ*Mtfkh1* mutant remains to be further investigated. Moreover, eighteen genes encoding transcription factors were also observed displaying altered expression levels in Δ*Mtfkh1* compared to WT, the majority of which possess unknown functions. Consequently, the increased production of cellulase and xylanase by mutant Δ*Mtfkh1* may also be the result of the combined effects of these putative transcriptional regulators. Based on our current knowledge, Pox08522 and MtFKH1 are, to date, the only two forkhead transcription factors known to regulate cellulase and xylanase biosynthesis in filamentous fungi. This implies that other uncharacterized proteins from the forkhead family in different fungal species may also play similar roles, warranting further exploitation.

MtFKH1 belongs to the forkhead protein family, which is evolutionarily conserved based on its forkhead box DNA-binding domain (DBD), and it exists widely from fungi to mammals. Like other classic transcription factors of lignocellulolytic enzyme gene expression, our EMSA analysis indicated that MtFKH1 could bind to the promoter regions of the main cellulase and xylanase genes. Previous study revealed that forkhead regulatory proteins shared the consensus motif 5′-G/A T/C C/A A A T/C A-3′ in the promoter regions of target genes (Kaufmann et al., 1995). For instance, StFKH1 of *S. cerevisiae* was found to bind to 5′-RYAAACAWW-3′ (Zhu et al., 2000), and Trident in mouse (FoxM1 in human) was capable of binding to TAAACA site (Korver et al., 1997; Laoukili et al., 2007). The DNase I footprinting assay demonstrated that MtFKH1 bound to 5′-CGGGAAGGCAAACATTGT-3′ in *bgl1*-p1, which displayed highest binding capacity with MtFKH1 during EMSA analyses, sharing the core motif recognized by other forkhead family members. Comparisons of different promoter regions of major cellulolytic and xylanolytic genes contributed to the discovery that AANYA is highly conserved in the promoter regions of target genes except for one of the assumptive binding sites ATCAATA of *bgl1*-p2. Additionally, the binding motifs in the *bgl1*-p3 showed one nucleotide variation compared to that in *bgl1*-p1, although increased predicted binding sites were observed in the *bgl1*-p3, which may help to explain that higher binding affinity detected between MtFKH1 and *bgl1*-p1. Similarly, the potential binding sequence of MtFKH1 in *cbh1*-p1 exhibited a nucleotide alteration relative to that in the *xyn1*-p3, which was consistent with the EMSA analysis that MtFKH1 prefer to bind to the promoter region of *xyn1*. These findings suggest that MtFKH1 directly regulates cellulase and xylanase production at the transcriptional level.

It has also been documented that forkhead proteins control cell development and morphogenesis. Knock-down of *Prfkh1* by RNAi (RNA interference) caused a 2.5-fold reduction in the number of spores compared with the control strain in *P. rubens*, although the hyphal morphology was unaffected (Dominguez-Santos et al., 2015). Likewise, deletion of *AnfkhB* displayed an impairment in conidiation under both light and dark conditions in *A. nidulans* (Jang et al., 2023). In *Magnaporthe oryzae*, loss of *Mofkh1* showed less effect on the number of conidia but resulted in decreased conidial germination compared to that of wild-type strain (Park et al., 2014). Also, deletion of both *fkh1* and *fkh2* exhibited pseudohyphal growth which was different from the nutritionally induced pseudohyphal phenotype in *S. cerevisiae* (Hollenhorst et al., 2000). The present study revealed that the Δ*Mtfkh1* mutant exhibited a 62 % reduction in spore production compared with the WT, further supporting the involvement of forkhead regulators in controlling fungal strain development. In filamentous fungi, the fungal development is tightly correlated with the activity of fungal velvet family proteins and the secondary metabolism regulator LaeA (Yu et al., 2024). Our transcriptomic data reflected that two important genes *MYCTH_113912* and *MYCTH_2294559*, which are predicted to be involved in cellular spore formation process, were downregulated ($\log_2$ fold change = −1.26 and −1.04, respectively) in Δ*Mtfkh1* mutant compared to the WT. MYCTH_113912 is the *M. thermophila* ortholog of the velvet family proteins velB in *A. nidulans* and vel2 in *T. reesei*. It was reported that velB in *A. nidulans* acts as a positive regulator of conidiation and deletion of *velB* caused decreased number of conidia and reduced and delayed transcript levels of several crucial asexual regulatory genes (Park et al., 2012). Similarly, in *T. reesei*, loss of *vel2* (the velB ortholog) resulted in sharp reduction of sporulation as well as downregulated expression of two key conidiation genes (Karimi Aghcheh et al., 2013; Liu et al., 2016). In addition, MYCTH_2294559 is orthologous to methyltransferase LaeA in *A. nidulans* and Lae1 in *T. reesei*. LaeA is a global regulator of secondary metabolism and participating in regulating growth, as well as sexual and asexual development in fungi (Bok and Keller, 2004; Karimi Aghcheh et al., 2013). The disruption of *lae1* substantially reduced sporulation, while overexpression of *lae1* resulted in increased sporulation in *T. reesei* (Seiboth et al., 2012). Likewise, LaeA is essential for the normal conidiation in *P. oxalicum*, as loss of which led to decreased levels of conidiation (Zhang et al., 2016). We, therefore, inferred that the decreased expression of genes encoding MtvelB and MtLaeA may cause sporulation defect in Δ*Mtfkh1* mutant.

The CRISPR/Cas9 genome editing is a powerful technique for accelerating in the manipulation of genes and pathways in fungal strains for manufacturing commodity chemicals and fuels with better yield (Pant et al., 2022; Shen et al., 2024). A CRISPR/Cas9 system was previously established in *M. thermophila*, generating multiple mutants with elevated lignocellulolytic enzymes production (Liu et al., 2017). In this study, we updated this system by integrating Cas9 protein and u6 promoter driven sgRNA in one expression vector, attempting to enhance the editing efficiency and make it labor-saving. We indeed obtained deletion strains for five potential regulatory genes, but the number of positive transformants differed. For example, two mutants for *MYCTH_2310243* were attained while only one stable mutant for MtFKH1 was gained. Moreover, three candidate TF genes failed to be disrupted by the CRISPR/Cas9 system, which was possibly due to the existence of lethal genes or inappropriate selection for protospacer sequences of target genes and/or low deletion efficacy of this CRISPR/Cas9 tool, indicating the genome editing system need to be further optimized to elevate the editing efficiency. Recently, new CRISPR/Cas12a and Base-Editing systems have been developed in *M. thermophila* (Liu et al., 2019c; Zhang et al., 2022), which should pave the way for identifying crucial regulators involved in plant biomass degradation and extend the toolkit for this fungal strain improvement.

Transcription factors play important roles in the regulation of cellulase and xylanase genes expression in filamentous fungi. In this study, we identified a novel forkhead transcription factor, MtFKH1, for the first time, which represses the cellulase and xylanase gene expression in *M. thermophila*. The deletion of regulatory repressor genes is a common genetic manipulation strategy to improve the production of extracellular enzymes. For example, simultaneous disruption of *cre1* and *res-1* resulted in higher secreted protein production and increased cellulase and xylanase activities in *M. thermophila* (Liu et al., 2017). The novel regulator MtFKH1 adds to the growing list of transcription factors that regulate cellulolytic and xylanolytic gene expression in *M. thermophila*, and offers a potential target for fungal genetic engineering. In *M. thermophila*, nearly all identified transcription factors

involved in regulating cellulase and/or hemicellulase production belong to either the zinc finger Zn2Cys6 type (Xyr1, Clr-2, Clr-4, Clr-5, Ara-1, AmyR) (Dos Santos Gomes et al., 2019; Gu et al., 2023) or the zinc finger C2H2 type (Cre1,TRC-1, Res-1) (Liu et al., 2017; Li et al., 2022) except for Hac-1, which is a basic-leucine zipper (bZIP) DNA-binding protein (Li et al., 2022). Thus, the characterization of MtFKH1 suggests that transcriptional regulators from other families besides zinc finger types in this fungus may also merit attention in the context of lignocellulose deconstruction.

5. Conclusion

In summary, the data of this study revealed that a new forkhead transcription factor MtFKH1 negatively regulates the expression of key cellulase and xylanase genes by directly binding to their promoter regions and is involved in controlling sporulation. This work expands the novel functions of the forkhead proteins in the regulation of genes encoding lignocellulosic biomass-degrading enzymes including cellulase and xylanase in *M. thermophila*, and could be useful for engineering of fungal strains with elevated cellulase and xylanase production capacity.

CRediT authorship contribution statement

Lai Yapeng: Writing – original draft, Visualization, Methodology, Investigation, Data curation, Conceptualization. **Wang Juan:** Supervision, Methodology, Funding acquisition, Conceptualization. **Xie Ning:** Methodology, Funding acquisition. **Liu Gang:** Writing – review & editing, Supervision, Methodology, Funding acquisition, Conceptualization. **Lacap-Bugler Donnabella Castillo:** Writing – review & editing, Supervision, Methodology, Conceptualization.

Declaration of Competing Interest

The authors declare no conflict financial interest.

Acknowledgements

This work was supported by the Natural Science Foundation of China (22078199 to Gang Liu), Natural Science Foundation of Guangdong Province (2024B1515020034), National Key R&D Program of China (2021YFA0910800 to Ning Xie), Shenzhen Municipal Science and Technology Basic Research Program (JCYJ20200109105210448 to Juan Wang), and Auckland University of Technology.

Appendix A. Supporting information

Supplementary data associated with this article can be found in the online version at doi:10.1016/j.micres.2025.128097.

Data availability

Data will be made available on request.

References

Adnan, M., Zheng, W., Islam, W., Arif, M., Abubakar, Y.S., Wang, Z., Lu, G., 2017. Carbon catabolite repression in filamentous fungi. Int J. Mol. Sci. 19 (1).
Adnan, M., Ma, X., Olsson, S., Wang, J., Liu, G., 2022. Promoter regulation and genetic engineering strategies for enhanced cellulase expression in Trichoderma reesei. Microbiol Res 259, 127011.
Agrawal, R., Verma, A., Singhania, R.R., Varjani, S., Di Dong, C., Kumar Patel, A., 2021. Current understanding of the inhibition factors and their mechanism of action for the lignocellulosic biomass hydrolysis. Bioresour. Technol. 332, 125042.
Ajeje, S.B., Hu, Y., Song, G., Peter, S.B., Afful, R.G., Sun, F., Asadollahi, M.A., Amiri, H., Abdulkhani, A., Sun, H., 2021. Thermostable cellulases / xylanases from thermophilic and hyperthermophilic microorganisms: current perspective. Front Bioeng. Biotechnol. 9, 794304.
Alazi, E., Ram, A.F.J., 2018. Modulating transcriptional regulation of plant biomass degrading enzyme networks for rational design of industrial fungal strains. Front Bioeng. Biotechnol. 6, 133.
Aro, N., Saloheimo, A., Ilmen, M., Penttila, M., 2001. ACEII, a novel transcriptional activator involved in regulation of cellulase and xylanase genes of Trichoderma reesei. J. Biol. Chem. 276 (26), 24309–24314.
Aro, N., Ilmen, M., Saloheimo, A., Penttila, M., 2003. ACEI of Trichoderma reesei is a repressor of cellulase and xylanase expression. Appl. Environ. Microbiol 69 (1), 56–65.
Bach, D.H., Long, N.P., Luu, T.T., Anh, N.H., Kwon, S.W., Lee, S.K., 2018. The dominant role of forkhead box proteins in cancer. Int J. Mol. Sci. 19 (10).
Bajaj, P., Mahajan, R., 2019. Cellulase and xylanase synergism in industrial biotechnology. Appl. Microbiol Biotechnol. 103 (21-22), 8711–8724.
Basotra, N., Kaur, B., Di Falco, M., Tsang, A., Chadha, B.S., 2016. Mycothermus thermophilus (Syn. Scytalidium thermophilum): repertoire of a diverse array of efficient cellulases and hemicellulases in the secretome revealed. Bioresour. Technol. 222, 413–421.
Benocci, T., Aguilar-Pontes, M.V., Zhou, M., Seiboth, B., de Vries, R.P., 2017. Regulators of plant biomass degradation in ascomycetous fungi. Biotechnol. Biofuels 10, 152.
Berka, R.M., Grigoriev, I.V., Otillar, R., Salamov, A., Grimwood, J., Reid, I., Ishmael, N., John, T., Darmond, C., Moisan, M.C., Henrissat, B., Coutinho, P.M., Lombard, V., Natvig, D.O., Lindquist, E., Schmutz, J., Lucas, S., Harris, P., Powlowski, J., Bellemare, A., Taylor, D., Butler, G., de Vries, R.P., Allijn, I.E., van den Brink, J., Ushinsky, S., Storms, R., Powell, A.J., Paulsen, I.T., Elbourne, L.D., Baker, S.E., Magnuson, J., Laboissiere, S., Clutterbuck, A.J., Martinez, D., Wogulis, M., de Leon, A.L., Rey, M.W., Tsang, A., 2011. Comparative genomic analysis of the thermophilic biomass-degrading fungi Myceliophthora thermophila and Thielavia terrestris. Nat. Biotechnol. 29 (10), 922–927.
Berlin, A., 2013. No barriers to cellulose breakdown. Science 342 (6165), 1454–1456.
Blumer-Schuette, S.E., Brown, S.D., Sander, K.B., Bayer, E.A., Kataeva, I., Zurawski, J.V., Conway, J.M., Adams, M.W., Kelly, R.M., 2014. Thermophilic lignocellulose deconstruction. FEMS Microbiol Rev. 38 (3), 393–448.
Bok, J.W., Keller, N.P., 2004. LaeA, a regulator of secondary metabolism in Aspergillus spp. Eukaryot. Cell 3 (2), 527–535.
Cai, P., Wang, B., Ji, J., Jiang, Y., Wan, L., Tian, C., Ma, Y., 2015. The putative cellodextrin transporter-like protein CLP1 is involved in cellulase induction in Neurospora crassa. J. Biol. Chem. 290 (2), 788–796.
Carlsson, P., Mahlapuu, M., 2002. Forkhead transcription factors: key players in development and metabolism. Dev. Biol. 250 (1), 1–23.
Chen, Y., Lin, A., Liu, P., Fan, X., Wu, C., Li, N., Wei, L., Wang, W., Wei, D., 2021. Trichoderma reesei ACE4, a novel transcriptional activator involved in the regulation of cellulase genes during growth on cellulose. Appl. Environ. Microbiol 87 (15), e0059321.
Coradetti, S.T., Craig, J.P., Xiong, Y., Shock, T., Tian, C., Glass, N.L., 2012. Conserved and essential transcription factors for cellulase gene expression in ascomycete fungi. Proc. Natl. Acad. Sci. USA 109 (19), 7397–7402.
Craig, J.P., Coradetti, S.T., Starr, T.L., Glass, N.L., 2015. Direct target network of the Neurospora crassa plant cell wall deconstruction regulators CLR-1, CLR-2, and XLR-1. mBio 6 (5), e01452–01415.
de Souza, W.R., de Gouvea, P.F., Savoldi, M., Malavazi, I., de Souza Bernardes, L.A., Goldman, M.H.S., de Vries, R.P., de Castro Oliveira, J.V., Goldman, G.H., 2011. Transcriptome analysis of Aspergillus niger grown on sugarcane bagasse. Biotechnol. Biofuels 4, 1–17.
Dominguez-Santos, R., Garcia-Estrada, C., Kosalkova, K., Prieto, C., Santamarta, I., Martin, J.F., 2015. PcFKH1, a novel regulatory factor from the forkhead family, controls the biosynthesis of penicillin in Penicillium chrysogenum. Biochimie 115, 162–176.
Dos Santos Gomes, A.C., Falkoski, D., Battaglia, E., Peng, M., Nicolau de Almeida, M., Coconi Linares, N., Meijnen, J.P., Visser, J., de Vries, R.P., 2019. Myceliophthora thermophila Xyr1 is predominantly involved in xylan degradation and xylose catabolism. Biotechnol. Biofuels 12, 220.
Eveleigh, D.E., Mandels, M., Andreotti, R., Roche, C., 2009. Measurement of saccharifying cellulase. Biotechnol. Biofuels 2, 21.
Ghose, T., 1987. Measurement of cellulase activities. Pure Appl. Chem. 59 (2), 257–268.
Gu, S., Zhao, Z., Xue, F., Liu, D., Liu, Q., Li, J., Tian, C., 2023. The arabinose transporter MtLat-1 is involved in hemicellulase repression as a pentose transceptor in Myceliophthora thermophila. Biotechnol. Biofuels Bioprod. 16 (1), 51.
Gupta, V.K., Kubicek, C.P., Berrin, J.G., Wilson, D.W., Couturier, M., Berlin, A., Filho, E. X.F., Ezeji, T., 2016. Fungal enzymes for bio-products from sustainable and waste biomass. Trends Biochem Sci. 41 (7), 633–645.
Hakkinen, M., Valkonen, M.J., Westerholm-Parvinen, A., Aro, N., Arvas, M., Vitikainen, M., Penttila, M., Saloheimo, M., Pakula, T.M., 2014. Screening of candidate regulators for cellulase and hemicellulase production in Trichoderma reesei and identification of a factor essential for cellulase production. Biotechnol. Biofuels 7 (1), 14.
Hollenhorst, P.C., Bose, M.E., Mielke, M.R., Muller, U., Fox, C.A., 2000. Forkhead genes in transcriptional silencing, cell morphology and the cell cycle. Overlapping and distinct functions for FKH1 and FKH2 in Saccharomyces cerevisiae. Genetics 154 (4), 1533–1548.
Jang, S.Y., Son, Y.E., Oh, D.S., Han, K.H., Yu, J.H., Park, H.S., 2023. The forkhead Gene fkhB is necessary for proper development in aspergillus nidulans. J. Microbiol Biotechnol. 33 (11), 1420–1427.
Juturu, V., Wu, J.C., 2014. Microbial cellulases: Engineering, production and applications. Renew. Sustain. Energy Rev. 33, 188–203.

Karimi Aghcheh, R., Druzhinina, I.S., Kubicek, C.P., 2013. The putative protein methyltransferase LAE1 of Trichoderma atroviride is a key regulator of asexual development and mycoparasitism. PLoS One 8 (6), e67144.
Karnaouri, A., Topakas, E., Antonopoulou, I., Christakopoulos, P., 2014. Genomic insights into the fungal lignocellulolytic system of Myceliophthora thermophila. Front Microbiol 5, 281.
Kaufmann, E., Muller, D., Knochel, W., 1995. DNA recognition site analysis of Xenopus winged helix proteins. J. Mol. Biol. 248 (2), 239–254.
Kim, D., Langmead, B., Salzberg, S.L., 2015. HISAT: a fast spliced aligner with low memory requirements. Nat. Methods 12 (4), 357–360.
Kjaergaard, C.H., Qayyum, M.F., Wong, S.D., Xu, F., Hemsworth, G.R., Walton, D.J., Young, N.A., Davies, G.J., Walton, P.H., Johansen, K.S., Hodgson, K.O., Hedman, B., Solomon, E.I., 2014. Spectroscopic and computational insight into the activation of O2 by the mononuclear Cu center in polysaccharide monooxygenases. Proc. Natl. Acad. Sci. USA 111 (24), 8797–8802.
Klaubauf, S., Narang, H.M., Post, H., Zhou, M., Brunner, K., Mach-Aigner, A.R., Mach, R. L., Heck, A.J.R., Altelaar, A.F.M., de Vries, R.P., 2014. Similar is not the same: differences in the function of the (hemi-)cellulolytic regulator XlnR (Xlr1/Xyr1) in filamentous fungi. Fungal Genet Biol. 72, 73–81.
Kolbusz, M.A., Di Falco, M., Ishmael, N., Marqueteau, S., Moisan, M.C., Baptista, C.D.S., Powlowski, J., Tsang, A., 2014. Transcriptome and exoproteome analysis of utilization of plant-derived biomass by Myceliophthora thermophila. Fungal Genet Biol. 72, 10–20.
Korver, W., Roose, J., Clevers, H., 1997. The winged-helix transcription factor Trident is expressed in cycling cells. Nucleic Acids Res 25 (9), 1715–1719.
Laissue, P., 2019. The forkhead-box family of transcription factors: key molecular players in colorectal cancer pathogenesis. Mol. Cancer 18 (1), 5.
Laoukili, J., Stahl, M., Medema, R.H., 2007. FoxM1: at the crossroads of ageing and cancer. Biochim Biophys. Acta 1775 (1), 92–102.
Li, B., Dewey, C.N., 2011. RSEM: accurate transcript quantification from RNA-Seq data with or without a reference genome. BMC Bioinforma. 12, 323.
Li, J., Lin, L., Li, H., Tian, C., Ma, Y., 2014. Transcriptional comparison of the filamentous fungus Neurospora crassa growing on three major monosaccharides D-glucose, D-xylose and L-arabinose. Biotechnol Biofuels. 7 (1), 31.
Li, J., Zhang, Y., Li, J., Sun, T., Tian, C., 2020a. Metabolic engineering of the cellulolytic thermophilic fungus Myceliophthora thermophila to produce ethanol from cellobiose. Biotechnol. Biofuels 13, 23.
Li, N., Liu, Y., Liu, D., Liu, D., Zhang, C., Lin, L., Zhu, Z., Li, H., Dai, Y., Wang, X., Liu, Q., Tian, C., 2022. MtTRC-1, a novel transcription factor, regulates cellulase production via directly modulating the genes expression of the mthac-1 and Mtcbh-1 in myceliophthora thermophila. Appl. Environ. Microbiol 88 (19), e0126322.
Li, X., Liu, Q., Sun, W., He, Q., Tian, C., 2020b. Improving cellulases production by Myceliophthora thermophila through disruption of protease genes. Biotechnol. Lett. 42 (2), 219–229.
Li, Y., Yan, P., Lu, X., Qiu, Y., Liang, S., Liu, G., Li, S., Mou, L., Xie, N., 2020c. Involvement of PaSNF1 in fungal development, sterigmatocystin biosynthesis, and lignocellulosic degradation in the filamentous fungus podospora anserina. Front Microbiol 11, 1038.
Li, Z., Yao, G., Wu, R., Gao, L., Kan, Q., Liu, M., Yang, P., Liu, G., Qin, Y., Song, X., Zhong, Y., Fang, X., Qu, Y., 2015. Synergistic and dose-controlled regulation of cellulase gene expression in penicillium oxalicum. PLoS Genet 11 (9), e1005509.
Liao, G.Y., Zhao, S., Zhang, T., Li, C.X., Liao, L.S., Zhang, F.F., Luo, X.M., Feng, J.X., 2018. The transcription factor TpRfx1 is an essential regulator of amylase and cellulase gene expression in Talaromyces pinophilus. Biotechnol. Biofuels 11, 276.
Liu, C.G., Xiao, Y., Xia, X.X., Zhao, X.Q., Peng, L., Srinophakun, P., Bai, F.W., 2019a. Cellulosic ethanol production: progress, challenges and strategies for solutions. Biotechnol. Adv. 37 (3), 491–504.
Liu, K., Dong, Y., Wang, F., Jiang, B., Wang, M., Fang, X., 2016. Regulation of cellulase expression, sporulation, and morphogenesis by velvet family proteins in Trichoderma reesei. Appl. Microbiol Biotechnol. 100 (2), 769–779.
Liu, P., Lin, A., Zhang, G., Zhang, J., Chen, Y., Shen, T., Zhao, J., Wei, D., Wang, W., 2019b. Enhancement of cellulase production in Trichoderma reesei RUT-C30 by comparative genomic screening. Micro Cell Fact. 18 (1), 81.
Liu, Q., Gao, R., Li, J., Lin, L., Zhao, J., Sun, W., Tian, C., 2017. Development of a genome-editing CRISPR/Cas9 system in thermophilic fungal Myceliophthora species and its application to hyper-cellulase production strain engineering. Biotechnol. Biofuels 10, 1.
Liu, Q., Li, J., Gao, R., Li, J., Ma, G., Tian, C., 2019d. CLR-4, a novel conserved transcription factor for cellulase gene expression in ascomycete fungi. Mol. Microbiol 111 (2), 373–394.
Liu, Q., Zhang, Y., Li, F., Li, J., Sun, W., Tian, C., 2019c. Upgrading of efficient and scalable CRISPR-Cas-mediated technology for genetic engineering in thermophilic fungus Myceliophthora thermophila. Biotechnol. Biofuels 12, 293.
Liu, Y.J., Li, B., Feng, Y., Cui, Q., 2020. Consolidated bio-saccharification: Leading lignocellulose bioconversion into the real world. Biotechnol. Adv. 40, 107535.
Livak, K.J., Schmittgen, T.D., 2001. Analysis of relative gene expression data using real-time quantitative PCR and the 2(-Delta Delta C(T)) Method. Methods 25 (4), 402–408.
Love, M.I., Huber, W., Anders, S., 2014. Moderated estimation of fold change and dispersion for RNA-seq data with DESeq2. Genome Biol. 15 (12), 550.
Ma, L., Chen, L., Zhang, L., Zou, G., Liu, R., Jiang, Y., Zhou, Z., 2016. RNA sequencing reveals Xyr1 as a transcription factor regulating gene expression beyond carbohydrate metabolism. Biomed. Res Int 2016, 4841756.
Makela, M.R., Donofrio, N., de Vries, R.P., 2014. Plant biomass degradation by fungi. Fungal Genet Biol. 72, 2–9.
Mansour, A.A., Da Costa, A., Arnaud, T., Lu-Chau, T.A., Fdz-Polanco, M., Moreira, M.T., Cacho Rivero, J.A., 2016. Review of lignocellulolytic enzyme activity analyses and scale-down to microplate-based assays. Talanta 150, 629–637.
Marui, J., Kitamoto, N., Kato, M., Kobayashi, T., Tsukagoshi, N., 2002. Transcriptional activator, AoXlnR, mediates cellulose-inductive expression of the xylanolytic and cellulolytic genes in Aspergillus oryzae. FEBS Lett. 528 (1-3), 279–282.
Mendonca, M., Barroca, M., Collins, T., 2023. Endo-1,4-beta-xylanase-containing glycoside hydrolase families: characteristics, singularities and similarities. Biotechnol. Adv. 65, 108148.
Morgenstern, I., Powlowski, J., Ishmael, N., Darmond, C., Marqueteau, S., Moisan, M.C., Quenneville, G., Tsang, A., 2012. A molecular phylogeny of thermophilic fungi. Fungal Biol. 116 (4), 489–502.
Nødvig, C.S., Nielsen, J.B., Kogle, M.E., Mortensen, U.H., 2015. A CRISPR-Cas9 system for genetic engineering of filamentous fungi. PLoS One 10 (7), e0133085.
Pant, S., Ritika, Nag, P., Ghati, A., Chakraborty, D., Maximiano, M.R., Franco, O.L., Mandal, A.K., Kuila, A., 2022. Employment of the CRISPR/Cas9 system to improve cellulase production in Trichoderma reesei. Biotechnol. Adv. 60, 108022.
Park, H.S., Ni, M., Jeong, K.C., Kim, Y.H., Yu, J.H., 2012. The role, interaction and regulation of the velvet regulator VelB in Aspergillus nidulans. PLoS One 7 (9), e45935.
Park, J., Kong, S., Kim, S., Kang, S., Lee, Y.H., 2014. Roles of forkhead-box transcription factors in controlling development, pathogenicity, and stress response in magnaporthe oryzae. Plant Pathol. J. 30 (2), 136–150.
Phillips, C.M., Beeson, W.T., Cate, J.H., Marletta, M.A., 2011. Cellobiose dehydrogenase and a copper-dependent polysaccharide monooxygenase potentiate cellulose degradation by Neurospora crassa. ACS Chem. Biol. 6 (12), 1399–1406.
Ries, L., Pullan, S.T., Delmas, S., Malla, S., Blythe, M.J., Archer, D.B., 2013. Genome-wide transcriptional response of Trichoderma reesei to lignocellulose using RNA sequencing and comparison with Aspergillus niger. BMC Genom. 14, 541.
Rubin, E.M., 2008. Genomics of cellulosic biofuels. Nature 454 (7206), 841–845.
Saloheimo, A., Aro, N., Ilmen, M., Penttila, M., 2000. Isolation of the ace1 gene encoding a Cys(2)-His(2) transcription factor involved in regulation of activity of the cellulase promoter cbh1 of Trichoderma reesei. J. Biol. Chem. 275 (8), 5817–5825.
Sanchez, C., 2009. Lignocellulosic residues: biodegradation and bioconversion by fungi. Biotechnol. Adv. 27 (2), 185–194.
Schmitt, E.K., Hoff, B., Kuck, U., 2004. AcFKH1, a novel member of the forkhead family, associates with the RFX transcription factor CPCR1 in the cephalosporin C-producing fungus Acremonium chrysogenum. Gene 342 (2), 269–281.
Seiboth, B., Karimi, R.A., Phatale, P.A., Linke, R., Hartl, L., Sauer, D.G., Smith, K.M., Baker, S.E., Freitag, M., Kubicek, C.P., 2012. The putative protein methyltransferase LAE1 controls cellulase gene expression in Trichoderma reesei. Mol. Microbiol 84 (6), 1150–1164.
Shen, Q., Ruan, H., Zhang, H., Wu, T., Zhu, K., Han, W., Dong, R., Ming, T., Qi, H., Zhang, Y., 2024. Utilization of CRISPR-Cas genome editing technology in filamentous fungi: function and advancement potentiality. Front Microbiol 15, 1375120.
Singh, B., 2016. Myceliophthora thermophila syn. Sporotrichum thermophile: a thermophilic mould of biotechnological potential. Crit. Rev. Biotechnol. 36 (1), 59–69.
Singhania, R.R., Sukumaran, R.K., Patel, A.K., Larroche, C., Pandey, A., 2010. Advancement and comparative profiles in the production technologies using solid-state and submerged fermentation for microbial cellulases. Enzym. Microb. Technol. 46 (7), 541–549.
Sperandio, G.B., Filho, E.X.F., 2021. An overview of Trichoderma reesei co-cultures for the production of lignocellulolytic enzymes. Appl. Microbiol Biotechnol. 105 (8), 3019–3025.
Stricker, A.R., Grosstessner-Hain, K., Wurleitner, E., Mach, R.L., 2006. Xyr1 (xylanase regulator 1) regulates both the hydrolytic enzyme system and D-xylose metabolism in Hypocrea jecorina. Eukaryot Cell. 5 (12), 2128-2137.
Sun, J., Glass, N.L., 2011. Identification of the CRE-1 cellulolytic regulon in Neurospora crassa. PLoS One 6 (9), e25654.
Sun, J., Tian, C., Diamond, S., Glass, N.L., 2012. Deciphering transcriptional regulatory mechanisms associated with hemicellulose degradation in Neurospora crassa. Eukaryot. Cell 11 (4), 482–493.
Taha, M., Foda, M., Shahsavari, E., Aburto-Medina, A., Adetutu, E., Ball, A., 2016. Commercial feasibility of lignocellulose biodegradation: possibilities and challenges. Curr. Opin. Biotechnol. 38, 190–197.
van Peij, N.N., Gielkens, M.M., de Vries, R.P., Visser, J., de Graaff, L.H., 1998. The transcriptional activator XlnR regulates both xylanolytic and endoglucanase gene expression in Aspergillus niger. Appl. Environ. Microbiol 64 (10), 3615–3619.
Visser, H., Joosten, V., Punt, P.J., Gusakov, A.V., Olson, P.T., Joosten, R., Bartels, J., Visser, J., Sinitsyn, A.P., Emalfarb, M.A., 2011. Development of a mature fungal technology and production platform for industrial enzymes based on a Myceliophthora thermophila isolate, previously known as Chrysosporium lucknowense C1. Ind. Biotechnol. 7 (3), 214–223.
Wang, B., Li, J., Gao, J., Cai, P., Han, X., Tian, C., 2017. Identification and characterization of the glucose dual-affinity transport system in Neurospora crassa: pleiotropic roles in nutrient transport, signaling, and carbon catabolite repression. Biotechnol. Biofuels 10, 17.
Wang, J., Wang, W., Wang, L., Zhang, G., Fan, K., Tan, H., Yang, K., 2011. A novel role of 'pseudo'gamma-butyrolactone receptors in controlling gamma-butyrolactone biosynthesis in Streptomyces. Mol. Microbiol 82 (1), 236–250.
Wang, J., Wu, Y., Gong, Y., Yu, S., Liu, G., 2015. Enhancing xylanase production in the thermophilic fungus Myceliophthora thermophila by homologous overexpression of Mtxyr1. J. Ind. Microbiol Biotechnol. 42 (9), 1233–1241.

Wang, Y., Cen, X.F., Zhao, G.P., Wang, J., 2012. Characterization of a new GlnR binding box in the promoter of amtB in Streptomyces coelicolor inferred a PhoP/GlnR competitive binding mechanism for transcriptional regulation of amtB. J. Bacteriol. 194 (19), 5237–5244.

Xie, S., Shen, B., Zhang, C., Huang, X., Zhang, Y., 2014. sgRNAcas9: a software package for designing CRISPR sgRNA and evaluating potential off-target cleavage sites. PLoS One 9 (6), e100448.

Xu, G., Li, J., Liu, Q., Sun, W., Jiang, M., Tian, C., 2018. Transcriptional analysis of Myceliophthora thermophila on soluble starch and role of regulator AmyR on polysaccharide degradation. Bioresour. Technol. 265, 558–562.

Xue, F., Zhao, Z., Gu, S., Chen, M., Xu, J., Luo, X., Li, J., Tian, C., 2023. The transcriptional factor Clr-5 is involved in cellulose degradation through regulation of amino acid metabolism in Neurospora crassa. BMC Biotechnol. 23 (1), 50.

Yang, F., Gong, Y., Liu, G., Zhao, S., Wang, J., 2015. Enhancing cellulase production in thermophilic fungus myceliophthora thermophila ATCC42464 by RNA interference of cre1 gene expression. J. Microbiol Biotechnol. 25 (7), 1101–1107.

Yeoman, C.J., Han, Y., Dodd, D., Schroeder, C.M., Mackie, R.I., Cann, I.K., 2010. Thermostable enzymes as biocatalysts in the biofuel industry. Adv. Appl. Microbiol 70, 1–55.

Yu, M., Zhou, X., Chen, D., Jiao, Y., Han, G., Tao, F., 2024. HacA, a key transcription factor for the unfolded protein response, is required for fungal development, aflatoxin biosynthesis and pathogenicity of Aspergillus flavus. Int J. Food Microbiol 417, 110693.

Zhang, C., Li, N., Rao, L., Li, J., Liu, Q., Tian, C., 2022. Development of an efficient C-to-T base-editing system and its application to cellulase transcription factor precise engineering in thermophilic fungus myceliophthora thermophila. Microbiol Spectr. 10 (3), e0232121.

Zhang, F., Zhao, X., Bai, F., 2018. Improvement of cellulase production in Trichoderma reesei Rut-C30 by overexpression of a novel regulatory gene Trvib-1. Bioresour. Technol. 247, 676–683.

Zhang, X., Zhu, Y., Bao, L., Gao, L., Yao, G., Li, Y., Yang, Z., Li, Z., Zhong, Y., Li, F., Yin, H., Qu, Y., Qin, Y., 2016. Putative methyltransferase LaeA and transcription factor CreA are necessary for proper asexual development and controlling secondary metabolic gene cluster expression. Fungal Genet Biol. 94, 32–46.

Zhao, S., Yan, Y.S., He, Q.P., Yang, L., Yin, X., Li, C.X., Mao, L.C., Liao, L.S., Huang, J.Q., Xie, S.B., Nong, Q.D., Zhang, Z., Jing, L., Xiong, Y.R., Duan, C.J., Liu, J.L., Feng, J.X., 2016. Comparative genomic, transcriptomic and secretomic profiling of Penicillium oxalicum HP7-1 and its cellulase and xylanase hyper-producing mutant EU2106, and identification of two novel regulatory genes of cellulase and xylanase gene expression. Biotechnol. Biofuels 9, 203.

Zhao, S., Liu, Q., Wang, J.X., Liao, X.Z., Guo, H., Li, C.X., Zhang, F.F., Liao, L.S., Luo, X. M., Feng, J.X., 2019. Differential transcriptomic profiling of filamentous fungus during solid-state and submerged fermentation and identification of an essential regulatory gene PoxMBF1 that directly regulated cellulase and xylanase gene expression. Biotechnol. Biofuels 12, 103.

Zhao, S., Zhang, T., Hasunuma, T., Kondo, A., Zhao, X.Q., Feng, J.X., 2023. Every road leads to Rome: diverse biosynthetic regulation of plant cell wall-degrading enzymes in filamentous fungi Penicillium oxalicum and Trichoderma reesei. Crit. Rev. Biotechnol. 1–21.

Zhu, G., Spellman, P.T., Volpe, T., Brown, P.O., Botstein, D., Davis, T.N., Futcher, B., 2000. Two yeast forkhead genes regulate the cell cycle and pseudohyphal growth. Nature 406 (6791), 90–94.

Znameroski, E.A., Li, X., Tsai, J.C., Galazka, J.M., Glass, N.L., Cate, J.H., 2014. Evidence for transceptor function of cellodextrin transporters in Neurospora crassa. J. Biol. Chem. 289 (5), 2610–2619.

Zou, G., Shi, S., Jiang, Y., van den Brink, J., de Vries, R.P., Chen, L., Zhang, J., Ma, L., Wang, C., Zhou, Z., 2012. Construction of a cellulase hyper-expression system in Trichoderma reesei by promoter and enzyme engineering. Micro Cell Fact. 11, 21.